Published in final edited form as:
Virology. 2013 November ; 446(0): 334–345. doi:10.1016/j.virol.2013.08.017.

Nuclear import of high risk HPV16 E7 oncoprotein is mediated by its zinc-binding domain via hydrophobic interactions with Nup62

Jeremy Eberhard, **Zeynep Onder**, and **Junona Moroianu***
Biology Department, Boston College, Chestnut Hill, MA 02467, USA

Abstract

We previously discovered that nuclear import of high risk HPV16 E7 is mediated by a cNLS located within the zinc-binding domain via a pathway that is independent of karyopherins/importins (Angeline et al., 2003; Knapp et al., 2009). In this study we continued our characterization of the cNLS and nuclear import pathway of HPV16 E7. We find that an intact zinc-binding domain is essential for the cNLS function in mediating nuclear import of HPV16 E7. Mutagenesis of cysteine residues to alanine in each of the two CysXXCys motifs involved in zinc-binding changes the nuclear localization of the EGFP-16E7 and 2xEGFP-16E7 mutants. We further discover that a patch of hydrophobic residues, $_{65}$**L**R**LCV**$_{69}$, within the zinc-binding domain of HPV16 E7 mediates its nuclear import via hydrophobic interactions with the FG domain of the central channel nucleoporin Nup62.

Introduction

Human Papillomaviruses (HPVs) are estimated to be the most common sexually transmitted infection in the United States. The largest group of HPVs are the alpha HPVs, and consists of both cutaneous viruses causing common warts, as well as the approximately 40 mucosal types known to infect the cervical epithelium. Mucosal HPVs are further divided into high and low risk groups, dependent upon the frequency with which they have been linked to the malignant progression of their resultant lesions (Doorbar, 2006; zur Hausen, 2000, 2009). Fifteen of the sexually transmitted genital HPVs can be classified as high risk, notably HPV16, HPV18, HPV31, HPV33 and HPV45, which may result in squamous intraepithelial lesions capable of progressing to invasive carcinomas (Doorbar, 2006; Munger et al., 2004; zur Hausen, 2000, 2009). Nearly 99% of cervical cancers and 20% of oropharynx cancers are positive for high risk HPV DNA, with HPV16 found in nearly 63% of the cervical cancers (Doorbar, 2006).

HPVs are dependent on the replication machinery of the host cells and consequently they have evolved the E7 oncoproteins to induce reentry into the S phase of the differentiated epithelial cells and establish the appropriate environment required to support viral DNA amplification. To accomplish this, the high risk HPV16/18 E7 oncoproteins bind and

*Correspondence about the manuscript, including proofs should be sent to: Junona Moroianu Boston College Biology Department, Higgins Hall, room 644B 140 Commonwealth Avenue Chestnut Hill, MA 02467 Tel: 617-552-1713 Fax: 617-552-2011 moroianu@bc.edu.

destabilize the retinoblastoma protein (pRB) and the RB-related pocket proteins, p130 and p107. E7 oncoproteins interact also with other components of the cell cycle machinery, such as cyclin A, cyclin E and the cyclin-dependent kinase inhibitors p27 and p21 (Jones and Munger,1996; Zwerschke and Jansen-Durr, 2000; McLaughlin-Drubin and Munger, 2009). In addition to these nuclear target proteins, HPV16 E7 binds to targets in the cytoplasm, such as the microtubule-associated N-end rule ubiqutin ligase p600 (Huh et al., 2005) and the nuclear mitotic apparatus protein (NuMA) (Nguyen and Munger, 2009).

Structurally, the E7 proteins consist of three biochemically distinct domains. Both NMR and X-ray crystal structures have been solved for the C terminal domain of E7, and the three-dimensional structure has been shown to organize into a tightly packed zinc-binding fold (McLaughlin-Drubin and Munger, 2009). The N terminus conserved regions (CR) CR1 (aa1-15) and CR2 (aa16-37) of HPV16 E7 possess significant sequence similarity to a portion of CR1 and the entirety of CR2 of adenovirus E1A and related sequences of SV40 large tumor antigen, as well as functional similarity, contributing to the transforming ability of HPV16 E7. The CR2 domain contains both the Leu-X-Cys-XGlu (LxCxE) pRB binding motif as well as a consensus casein kinase II (CKII) phosphorylation site. The C-terminal CR3 domain (aa38-98) contains a zinc-binding domain with two Cys-X-X-Cys motifs separated by 29 amino acids (McLaughlin-Drubin and Munger, 2009).

High risk HPV16 E7 is predominantly nuclear in the CaSki cervical carcinoma cell line, when expressed transiently in HaCaT and U2OS cells, and in invasive cervical carcinoma (Guccione et al., 2002; Fiedler et al., 2004; Cid-Arregui et al., 2003). We have previously discovered that nuclear import of HPV16 E7 and HPV11 E7 is mediated by a Ran-dependent pathway that is independent of karyopherins/importins and it is mediated by their cNLS located within the unique zinc-binding domain (Angeline et al., 2003; Knapp et al., 2009; Piccioli et al., 2010). Both HPV16 E7 and HPV11 E7 proteins have also a leucine-rich nuclear export signal (NES) located within the zinc-binding domain that mediates their nuclear export via a CRM1 pathway (Knapp et al., 2009; McKee et al., 2013).

Nuclear import and export of different cargoes take place through nuclear pore complexes (NPCs) embedded at the nuclear envelope. There are some 30 nucleoporins (Nups) that assemble to form the NPC and they can be classified into: transmembrane Nups (Poms) that anchor the NPCs at the nuclear envelope, structural Nups, and FG-Nups containing phenylalanine-glycine (FG) repeats, and involved in nuclear import and export (Terry and Wente, 2009). Transport through the NPCs can be via passive diffusion for cargoes up to approximately 40 kDa, active transport mediated by karyopherins (importins and exportins) interacting with FG-Nups for cargoes over 40 kDa, and direct interaction of some cargoes with FG-Nups bypassing the requirement for karyopherins (Terry and Wente, 2009). The central channel for nucleocytoplasmic transport consists of three nucleoporins, Nup62, Nup58 and Nup54 and the structures of the Nup62-Nup54 and Nup54-Nup58 interacting domains has been recently determined revealing the architecture of the mammalian transport channel (Solmaz et al., 2011).

In this study we continue our characterization of the cNLS and nuclear import pathway of high risk HPV16 E7 oncoprotein. We determine that an intact zinc-binding domain within the CR3 domain is essential for the cNLS function in mediating nuclear import of HPV16 E7. Mutagenesis of Cys residues in each of the two CysXXCys motifs involved in zinc binding changes the nuclear localization of the resultant EGFP-16E7 and 2xEGFP-16E7 mutants. We further discover that a patch of hydrophobic residues, $_{65}$**LRLCV**$_{69}$, within the zinc-binding domain of HPV16 E7 mediates its nuclear import via direct hydrophobic interactions with the FG domain of the channel nucleoporin, Nup62.

Results

The zinc-binding domain of HPV16 E7 is essential for its nuclear localization

We have previously established the presence of a C-terminal NLS in the CR3 domain of HPV16 E7 containing the zinc-binding fold that consists of two copies of a Cys-X-X-Cys motif separated by 29 amino acids (Knapp et al., 2009). Moreover, we have determined that the zinc-binding domain of HPV11 E7 is essential for its nuclear import and localization (Piccioli et al., 2010). To examine the possibility that the intact zinc-binding domain of HPV16 E7 is essential for the nuclear import activity of the cNLS of HPV16 E7 we have now performed site-directed mutagenesis of cysteine residues in each of the two copies of Cys-X-X-Cys in the context of EGFP-16E7 and 2xEGFP-16E7 generating the CC58/59AA and C91A mutants. The CC58/59AA mutant is designated CC58AA for simplicity. HeLa cells were transiently transfected with the wild type EGFP-16E7, the EGFP-16E7$_{CC58AA}$ and EGFP-16E7$_{C91A}$ cysteine mutants and EGFP control, and the cellular localization of the expressed proteins was examined via confocal fluorescence microscopy. As previously reported, the wild type EGFP-16E7 had a nuclear localization in the majority of transfected cells with the rest of cells having a pancellular phenotype (Fig. 1); EGFP had a pancellular localization in all the transfected cells (Fig. 1). Both the EGFP-16E7$_{CC58AA}$ and EGFP-16E7$_{C91A}$ cysteine mutants exhibited a pancellular localization, similar with that of EGFP, in the majority of transfected cells, 83.2% +/− 4.1%, and 85.8% +/− 6.9% respectively (Fig. 1). These data indicate that, while disruption of the zinc-binding domain in the context of EGFP-16E7 led to a change in the localization from mostly nuclear to pancellular, it did not completely prevent the EGFP-16E7$_{CC58AA}$ or EGFP-16E7$_{C91A}$ mutants from gaining some entry to the nucleus. As the cysteine mutations can affect the dimerization of 16E7, and in the absence of dimerization the EGFP-16E7$_{CC58AA}$ and EGFP-16E7$_{C91A}$ mutants could enter by passive diffusion (as the EGFP itself), we generated the same mutants in the context of 2xEGFP-16E7 (containing a 2xEGFP module) to exceed the limit for passive diffusion across the nuclear pore complex. HeLa cells were transiently transfected with the 2xEGFP-16E7$_{CC58AA}$ and 2xEGFP-16E7$_{C91A}$ mutants, along with the 2xEGFP-16E7 wild type and 2xEGFP control. As previously reported the 2xEGFP-16E7 wild type had a predominantly nuclear localization in the majority of cells (Fig. 1 and Fig. 2, panels B and C) and 2xEGFP had a cytoplasmic localization (Fig. 1 and Fig. 2, panels K and L). Significantly, the 2xEGFP-16E7$_{CC58AA}$ and 2xEGFP-16E7$_{C91A}$, exhibited predominantly cytoplasmic localization in the majority of transfected cells, 86.4% +/− 3.6% and 89.8% +/− 5.1%, respectively (Fig. 1 and Fig. 2, panels E, F, H and I). Together these data support the conclusion that the nuclear import activity of the cNLS of HPV16 E7 is dependent upon an intact zinc-binding domain. The loss of zinc coordination in the cysteine mutants can lead to structural changes in the zinc-binding domain that would make unavailable the critical residues of the cNLS.

We have previously showed that a cysteine residue at position 59 - conserved between the high risk and low risk HPVs, and not involved in coordinating the zinc ion - plays some role in the cNLS function of HPV11 E7 (Piccioli et al., 2010). To examine if this conserved cysteine residue performs a similar function in HPV16 E7, site directed mutagenesis was used to generate a pair of single amino acid substitutions of the N-terminal cysteines within the zinc-binding domain in the context of 2xEGFP-16E7. The 2xEGFP-16E7 wild type, 2xEGFP-16E7 single cysteine mutants and 2xEGFP, were transiently transfected into HeLa cells and their resultant subcellular localizations were examined via confocal fluorescence microscopy. Both 2xEGFP-16E7 wild type and 2xEGFP-16E7$_{C59A}$ exhibited predominantly nuclear localization (Fig. 3A, panels B and C; and panels H and I), although at reduced levels for the 2xEGFP-16E7$_{C59A}$ mutant (57.3% +/− 11.1%) (Fig. 3B). In contrast, the 2xEGFP-16E7$_{C58A}$ exhibited predominantly pancellular localization (Fig. 3A, panels E, and F) in 66.3% +/− 18.6% cells and also cytoplasmic localization in 28.8% +/−18.8% cells

(Fig. 3B). In the context of 1xEGFP, the reductions in nuclear localization caused by the C58A and C59A mutations were more modest. EGFP-16E7$_{C58A}$ and EGFP-16E7$_{C59A}$ were predominantly nuclear in 55.3% +/− 5.7% and 69.3% +/−9.5% transfected cells with the rest of cells exhibiting a pancellular phenotype (Fig. 3B); this is in comparison with 85% +/− 2.4% cells showing nuclear localization for the EGFP-16E7 wild type (Fig. 3B). Immunoblot analyses of the expressed EGFP-16E7, 2xEGFP-16E7 and the different cysteine mutants performed with a GFP antibody indicated that the wild type and mutant proteins were expressed properly at similar levels (Fig. 4). These data suggest that cysteine 59 can partially compensate for the loss of cysteine 58 in coordinating the zinc ion and maintaining the zinc-binding domain and nuclear localization, and also that cysteine 59 may play a very modest role in the cNLS function.

A hydrophobic patch within the zinc-binding domain is essential for the nuclear localization of HPV16 E7

The surface hydrophobicity of karyopherins/importins is sufficient to provide access to the NPC and translocation is achieved through a series of non-specific interactions between short hydrophobic patches on the surface of the karyopherins and the FG-Nups within the NPC (Naim et al., 2009). We have previously identified a small hydrophobic patch of amino acids, $_{65}$**VRLVV**$_{69}$, within the zinc-binding domain of HPV11 E7 that was required for its nuclear localization (McKee et al., 2013). A small hydrophobic patch within the zinc-binding domain of HPV16 E7, $_{65}$**LRLCV**$_{69}$, has significant homology to the patch previously characterized in HPV11 E7, **$_{65}$VRLVV$_{69}$** (McKee et al., 2013). To examine the possibility that this hydrophobic patch of amino acids within the zinc-binding domain of HPV16 E7 is required for mediating its nuclear import we used site-directed mutagenesis to replace all five amino acids with alanine and generated the LRLCV65-69AAAAA mutation in the context of 2xEGFP-16E7 and GST-16cE7. The LRLCV65-69AAAAA mutation is designated LRLCV65AAAAA, again for simplicity. We also generated single mutants by substituting the arginine at position 66 with alanine in the context of 2xEGFP-16E7 and GST-16cE7.

HeLa cells were transiently transfected with the 2xEGFP-16E7$_{LRLCV65AAAAA}$ and 2xEGFP-16E7$_{R66A}$ mutants, along with the 2xEGFP-16E7 wild type and 2xEGFP and the localization of the resultant proteins was examined via confocal fluorescence microscopy. As previously shown the 2xEGFP-16E7 wild type was nuclear in the majority of cells (Fig. 5A, panels E and I; and Fig. 5B) whereas the 2xEGFP was cytoplasmic in all the transfected cells (Fig. 5A, panels H and L; and Fig. 5B). In contrast with the nuclear localization of the wild type, the 2xEGFP-16E7$_{LRLCV65AAAAA}$ mutant was cytoplasmic in 84.9% +/− 4.3% of transfected cells, with the rest of cells having a pancellular localization (Fig. 5A, panels F and J; and Fig. 5B). The 2xEGFP-16E7$_{R66A}$ mutant had a similar nuclear localization as the wild type in the majority of cells (86.2% +/− 4.2%) (Fig. 5A, panels G and K; and Fig. 5B). In the context of EGFP-16E7, 84.8% +/− 4.2% of EGFP-16E7$_{LRLCV65AAAAA}$ expressing cells exhibited a pancellular phenotype similarly as the EGFP itself (Fig. 5C), whereas 92.3% +/− 2.6% of EGFP-16E7$_{R66A}$ expressing cells exhibited a predominantly nuclear phenotype (Fig. 5C). Together these data suggest that these hydrophobic residues, $_{65}$**LRLCV**$_{69}$, are responsible for the nuclear localization of 2xEGFP-16E7 and EGFP-16E7 whereas the positively charged arginine 66 residue plays no significant role in the function of the cNLS. To ensure that the results observed were not due to degradation of the mutants, immunoblot analysis with an anti-GFP antibody was performed. The data indicate that all the 2xEGFP-16E7 and EGFP-16E7 mutant proteins were expressed at the correct molecular weight and at similar levels with their corresponding wild type proteins; although the 2xEGFP-16E7 mutants show a certain level of proteolytic degradation, it is at the same level as for the 2xEGFP-16E7 wild type (Fig. 5D).

To further confirm this conclusion drawn from the transient transfection experiments in HeLa cells, *in vitro* nuclear import assays were performed using the same mutants in the context of GST-16cE7. In these experiments, digitonin permeablized HeLa cells were incubated with GST-16cE7, GST-16cE7$_{LRLCV65AAAAA}$, GST-16cE7$_{R66A}$, GST-M9 as a positive control, or GST as a negative control, in the presence of either transport buffer or HeLa cytosol. Detection of the GST fusion proteins was via immunofluorescence staining with a specific GST antibody and subsequent examination by confocal fluorescence microscopy. As expected, both GST-16cE7 and GST-M9 were imported into the nucleus in the presence of HeLa cytosol (Fig. 6, panels G and F). In agreement with the previous transfection data the GST-16cE7$_{LRLCV65AAAAA}$ hydrophobic mutant was no longer imported into the nucleus, whereas the GST-16cE7$_{R66A}$ was imported into the nucleus in the presence of cytosol (Fig. 6, panels H and I). As expected, no nuclear import was observed for the GST negative control (Fig. 6, panel J). Together these data support the previous conclusion that the hydrophobic residues, $_{65}$**LRLCV**$_{69}$, within the zinc-binding domain of HPV16 E7 are essential for the cNLS function and that the charged arginine residue at position 66 has no significant role in nuclear import.

HPV16 E7 interacts via its zinc-binding domain with the FG domain of Nup62

The mechanism by which hydrophobic residue patches of karyopherins mediate nuclear import is through non-specific hydrophobic interactions with the FG repeats in nucleoporins (Terry and Wente, 2009). To examine the possibility that the hydrophobic patch of HPV16 E7, $_{65}$**LRLCV**$_{69}$, mediates nuclear import through direct non-specific interactions with FG-Nups we performed isolation assays. For these experiments we chose the FG nucleoporin Nup62 because it is located at the central transport channel of the NPC and interacts with karyopherins/importins mediating nucleocytoplasmic traffic of cargoes (Solmaz et al., 2011). Nup62 forms triple helices with Nup54 that project alternatively up and down from either side of the midplane Nup54-Nup58 ring, and constitute cytoplasmic and nucleoplasmic entries for nuclear import and export complexes via their N-terminal FG domains (Solmaz et al., 2011). In these experiments we used GST-Nup62N, containing all six FG repeats of Nup62, and GST, as a negative control. These GST fusion proteins were immobilized on glutathione-Sepharose beads and incubated with HeLa cell lysates expressing EGFP-16E7 wild type, EGFP-16E7$_{LRLCV65AAAAA}$, EGFP-16E7$_{R66A}$, or EGFP. The bound proteins were then eluted and analyzed via immunoblotting with a GFP antibody. As a positive control for binding to Nup62N we used Kap β2/transportin. The positive control, Kap β2 bound to GSTNup62N (Fig. 7, lane 10) but not to GST itself (Fig. 7, lane 15), whereas the negative control EGFP did not bind to either one (Fig. 7, lanes 9 and 14). Significantly, the results show that both EGFP-16E7 wild type and EGFP-16E7$_{R66A}$ interacted with GST-Nup62N (Fig. 7, lanes 6 and 8), but not with GST (Fig. 7, lanes 11 and 13, respectively). This correlates well with the previously observed nuclear localization of both EGFP-16E7 and EGFP-16E7$_{R66A}$. Significantly, the EGFP-16E7$_{LRLCV65AAAAA}$ hydrophobic residue mutant failed to interact with GST-Nup62N (Fig. 7, lane 7). We also performed isolation assays with GST-Nup62C, representing the C- terminal domain of Nup62 lacking any FG repeats, and neither Kap β2 nor EGFP-16E7 bound to GST-Nup62C (data not shown). Taken together, these data strongly suggest that the patch of hydrophobic residues, $_{65}$**LRLCV**$_{69}$, within the zinc-binding domain of HPV16 E7 is essential for the cNLS function through the interaction with the FG repeats in Nup62, and that the charged arginine residue at position 66 has no role in this process.

Interestingly, an HPV16 E7 mutant containing a mutation in this mostly hydrophobic patch L67R, although retaining its ability to bind pRb, is defective in abrogating pRB-mediated cell cycle arrest and fails to bind HDAC (Avvakumov et al., 2003; Brehm et al., 1999). To examine if this L67R mutation within $_{65}$**LRLCV**$_{69}$ interferes with the nuclear localization of

HPV16 E7 we introduced this mutation both in the context of EGFP-16E7 and 2xEGFP-16E7 and analyzed their localization in comparison with the wild type proteins. In contrast with the nuclear localization of EGFP-16E7 and 2xEGFP-16E7 (Fig. 8A, panels A and I; panels C and K; and Fig. 8B), the EGFP-16E7$_{L67R}$ had a pancellular localization in 85.8 +/− 0.9 % of transfected cells (Fig. 8A, panels B and J; and Fig. 8B), whereas the 2xEGFP-16E7$_{L67R}$ had a cytoplasmic localization in 76.8 +/− 2.5% of cells and a pancellular localization in the rest of cells (Fig. 8A, panels D and L; and Fig. 8B). Immunoblot analysis with an anti-GFP antibody indicated that EGFP-16E7$_{L67R}$ and 2xEGFP-16E7$_{L67R}$ mutant proteins were expressed at the correct molecular weight and at similar levels with their corresponding wild type proteins (Fig. 8C). These results indicate that the hydrophobic leucine 67 residue is essential for the nuclear localization of 16E7 and its substitution with the positively charged arginine residue leads to a loss of nuclear import function of the cNLS.

There is another HPV16 E7 mutant that partially overlaps with the $_{65}$**L**R**LCV**$_{69}$ hydrophobic patch, CVQ68-70AAA, that has a mixed phenotype: it has wild type activity regarding the ability to block binding of pRb to E2F and to destabilize pRb (Helt and Galloway, 2001), and to bind to p600 and E2F6 (Huh et al., 2005; McLaughlin-Drubin et al., 2008); however, the CVQ68-70AAA mutant fails to bypass DNA damage checkpoints, to extend HFK lifespan, to inactivate p21 and to bind to cullin 2 ubiquitin ligase complex (Helt and Galloway, 2001; Helt et al., 2002; Huh et al., 2007; Roman and Munger, 2013). We generated the 2xEGFP-16E7$_{CVQ68AAA}$ mutant and analyzed its localization in comparison with the wild type and found that the CVQ68-70AAA mutation caused a change in the localization from nuclear in the majority of cells (85.65% +/− 7.2%) for the wild type to pancellular in 61.83% +/− 4.4% of cells and cytoplasmic in 35.73% +/− 4.17% cells for the mutant (Fig. 9A). These data indicate that substitution of the last two residues in the hydrophobic patch, cysteine and valine, to alanine leads to significant weakening of the cNLS nuclear import function.

Discussion

In this study we continued our analysis of the nuclear import pathway and characterization of the cNLS of high risk HPV16 E7 using both transfection assays in HeLa cells with EGFP fusions containing 16E7 and different mutants and nuclear import assays in digitonin-permeabilized HeLa cells with GST fusions to the CR3 of 16E7. The CR3 domain contains a zinc-binding domain that consists of two Cys-X-X-Cys motifs separated by 29 amino acids that is conserved between the high and low risk HPV types (McLaughlin-Drubin and Munger, 2009). The integrity of this zinc-binding domain has been shown to be necessary for dimerization and, in high risk HPV types, the transformative capacity of E7 (McLaughlin-Drubin and Munger, 2009). Here we presented data showing that mutations of Cys residues in the two Cys-X-X-Cys motifs that affect the zinc binding clearly disrupt the nuclear localization of the resultant EGFP-16E7 and 2xEGFP-16E7 mutants. These data strongly suggest that the integrity of the zinc-binding domain of HPV16 E7 is critical for the nuclear import activity of the cNLS, in addition to the requirement for dimerization and transformation potential. The cysteine residues involved in zinc coordination within the CR3 domain of E7 proteins are the most highly conserved cysteine residues among the different HPV types and we have previously established for the low risk HPV11 E7 that the integrity of its zinc-binding domain is essential for the nuclear import activity of the cNLS (Piccioli et al., 2010). The loss of zinc coordination can lead to structural changes of the CR3 domain that would make unavailable the critical hydrophobic residues of the cNLS. In addition, another viral protein, the TAX protein of human T lymphotropic virus type 1 (HTLV-1), also enters the nucleus via a pathway mediated by its zinc-binding domain (Tsuji et al., 2007).

Our previous studies have shown that nuclear entry of HPV16 E7 is mediated by its unique cNLS using a pathway that it is independent of karyopherins/importins (Angeline et al., 2003; Knapp et al., 2009). One possible mechanism that bypasses the requirement of nuclear import receptors is via direct low affinity hydrophobic interactions between E7 and the phenylalanine-glycine (FG) repeats in FG nucleoporins in a manner similar to that used by traditional receptors/karyopherins. Significantly, the zinc-binding domain of HPV16 E7 is very rich in nonpolar hydrophobic residues, with some of them arranged in small hydrophobic patches, suggesting a similar mechanism for how the zinc-binding domain of HPV16 E7 is able to mediate nuclear import. In this study we determined that HPV16 E7 interacts via its zinc-binding domain with the FG repeats domain of Nup62, a nucleoporin located at the central channel of the NPC and involved in nuclear import and export of cargoes (Solmaz et al., 2011). Significantly, we found a mostly hydrophobic patch, $_{65}$**L**R**LCV**$_{69}$, within the zinc-binding domain that is essential for the nuclear localization of EGFP-16E7 and 2xEGFP-16E7. Mutation of the hydrophobic residues to alanine was sufficient to disrupt the predominantly nuclear localization of EGFP-16E7 and 2xEGFP-16E7 and inhibit the nuclear import of GST-16cE7 in digitoninpermeabilized cells. In contrast, no change in localization was observed in either the transfection assays, or the nuclear import assays by mutating the arginine 66 residue to alanine, suggesting that this positively charged residue has no role in the nuclear import of HPV16 E7. Significantly, mutation of the hydrophobic residues to alanine inhibited the interaction of HPV16 E7 with the FG domain of Nup62, suggesting that the hydrophobic residues of this sequence play a critical role in facilitating the interaction of the zinc-binding domain of HPV16 E7 with Nup62. Based on the structure of the zinc-binding domain dimer of HPV1A E7 and the sequence alignment with other E7 proteins, the $_{65}$**L**R**LCV**$_{69}$ patch is located on the β2 strand and **L**65**, L**67 and **V**69 are highly conserved hydrophobic residues and may participate in hydrophobic interactions that stabilize the dimer (Liu et al., 2006). Interestingly, an HPV16 E7 L67R mutant, although it binds pRb *in vitro*, fails to overcome cell cycle arrest in osteosarcoma cells *in vivo* and to transactivate E2F-dependent promoters (Avvakumov et al., 2003; Brehm et al., 1999). As this L67R mutation within the hydrophobic patch involved in nuclear import of HPV16 E7 disrupts 16E7 nuclear localization, it can be speculated that this may contribute to the phenotype of the mutant *in vivo*. Another HPV16 E7 mutant, that partially overlaps with the hydrophobic patch, CVQ68-70AAA, fails to bypass DNA damage checkpoints, to extend HFK lifespan and to inactivate p21 (Helt and Galloway, 2001; Helt et al., 2002). The CVQ68-70AAA mutation decreases the nuclear localization and increases the cytoplasmic localization of 16E7, which may contribute to some of its loss of function(s). The R66A mutant, that retains the nuclear localization of the wild type, also retains the wild type phenotype, the ability to destabilize pRb and to bypass DNA damage checkpoints (Helt and Galloway, 2001).

Overall, the data strongly suggest that the cNLS mediated nuclear import of HPV16 E7 is via non-specific hydrophobic interactions of its zinc-binding domain with the FG repeats domain of Nup62 at the NPC. The mechanism of nuclear import of high risk HPV16 E7 oncoprotein is conserved with that of low risk HPV11 E7 protein (McKee et al., 2013). Nuclear import of HPV11 E7 is mediated by direct interactions between a homologous hydrophobic patch, $_{65}$**V**R**LVV**$_{69}$, within the zinc-binding domain with the FG domain of Nup62 (McKee et al., 2013). Also, the cutaneous high risk HPV8 E7 enters the nucleus via hydrophobic interactions between a homologous hydrophobic patch, $_{65}$**L**R**LFV**$_{69}$, with the FG domain of Nup62 (manuscript in preparation). It is likely that HPV E7 proteins might interact with other FG nucleoporins like Nup153 and Nup54 during their translocation through the NPC into the nucleus.

While the mechanism of nuclear import of HPV E7 oncoproteins is conserved between different HPV types, it is unique in comparison to other HPV proteins, including the L1 and

L2 capsid proteins and the E6 oncoprotein that use different karyopherins to enter the nucleus (Bordeaux et al., 2006; Darshan et al., 2004; Klucevsek et al., 2006; Le Roux and Moroianu, 2003; Nelson et al., 2002). We can only speculate at this time why the HPV E7 proteins have evolved this nuclear import mechanism independent of karyopherins, but the relatively small size, the richness in hydrophobic residues and the relative low concentration may favor direct interaction of the E7 proteins with FG nucleoporins and bypassing the competition for karyopherins. An interesting possibility, that remains to be explored, is that E7 may also function as a carrier facilitating the nuclear import of a cellular target protein and changing its nucleocytoplasmic distribution.

Another viral oncoprotein, the TAX protein of HTLV-1 also enters the nucleus via direct hydrophobic interactions of its zinc-binding domain with the FG nucleoporin Nup62 at the NPC (Tsuji et al., 2007). Also, a cellular protein, like PU.1 transcription factor, enters the nucleus independent of karyopherins via direct binding to the FG nucleoporins, Nup62 and Nup153 (Zhong et al., 2005).

Materials and methods

Mutagenesis to generate different EGFP-16E7 and 2xEGFP-16E7 mutants

EGFP-16E7 and 2xEGFP-16E7 plasmids were obtained previously (Knapp et al., 2009). The cysteine mutants EGFP-16E7$_{C58A}$, 2xEGFP-16E7$_{C58A}$, EGFP-16E7$_{CC58AA}$, 2xEGFP-16E7$_{CC58AA}$, EGFP-16E7$_{C91A}$, 2xEGFP-16E7$_{C91A}$, EGFP-16E7$_{C59A}$, and 2xEGFP-16E7$_{C59A}$ mutants were generated using the QuikChange™ Site-Directed Mutagenesis Kit (Stratagene) with either EGFP-16E7 or 2xEGFP-16E7 as templates, and the corresponding mutagenesis primer pairs.

The EGFP-16E7$_{LRLCV65AAAAA}$, 2xEGFP-16E7$_{LRLCV65AAAAA}$, EGFP-16E7$_{R66A}$, 2xEGFP-16E7$_{R66A}$, EGFP-16E7$_{L67R}$, 2xEGFP-16E7$_{L67R}$ and 2xEGFP-16E7$_{CVQ68AAA}$ mutants were generated using the QuikChange™ Site-Directed Mutagenesis Kit with either EGFP-16E7 or 2xEGFP-16E7 as templates, and the corresponding mutagenesis primer pairs.

All mutant plasmids were transformed into XL1-Blue competent cells (Agilent Technologies), purified and sequenced for verification (Eurofins MWG).

Transient expression of EGFP fusion proteins and confocal microscopy analysis

HeLa cells (ATCC) were plated on 12 mm poly-L-lysine-coated glass coverslips to 50 % confluency 24 h prior to transfection. Cells in each well were transfected with the corresponding EGFP fusion plasmid (as indicated in the figure legends) and the FuGENE 6 reagent (Roche Applied Science, IN). Media was changed to DMEM with 10% FBS and 1% penicillin-streptomycin after 6 h and the cells were fixed 24 h after the initial transfection with 3.7% formaldehyde in PBS (10 min). Coverslips were mounted using Vectashield-DAPI mounting medium (Vector Labs, CA) to visualize the nuclei by DAPI staining. The slides were examined by confocal fluorescence microscopy using a Leica TCS Sp5 broadband confocal microscope and pictures were taken using the Leica LAS AF software (Leica Microsystems).

Intracellular localization phenotypes of the different EGFP fusion proteins were scored as predominantly nuclear, pancellular, or predominantly cytoplasmic, as visually observed via confocal fluorescence microscopy for each of the transfection experiments. Data from four to seven experiments (as indicated in the figure legends) were used for quantitative analysis. The graphical representations for each quantitative analysis display average values with standard deviations. Immunoblot analyses of the expressed EGFP-16E7, 2xEGFP-16E7 and

different mutants performed with a GFP antibody indicated that the proteins were expressed at similar levels and not degraded.

Preparation of GST-16cE7 Mutant Proteins—The GST-16cE7 plasmid was obtained previously (Knapp et al., 2009). The GST-16cE7$_{R66A}$ and GST-16cE7$_{LRLCV65AAAAA}$ mutants were generated using the QuikChange™ Site-Directed Mutagenesis Kit with GST-16cE7 as the template, and the mutagenesis primer pairs as indicated above. The mutant plasmids were transformed into XL1-Blue competent cells and extracted using Quantum Prep® Plasmid MidiPrep kit. All purified plasmids were sequenced for verification (Eurofins MWG).

For protein expression and purification, each GST-16cE7 plasmid was used to transform E. coli BL21 CodonPlus (Agilent Technologies). Bacteria were then induced with 1mM IPTG for 3 h at 37°C, and each mutant protein was purified in its native state on glutathione-Sepharose beads (GE Healthcare) using a standard procedure. The GST-M9 positive control containing the NLS of hnRNPA1 was also prepared on glutathione-Sepharose beads using a standard procedure. All purified GST fusion proteins were dialyzed in transport buffer (20 mM HEPES-KOH pH 7.3, 110mM potassium acetate, 2 mM magnesium acetate, 1 mM EGTA, and 2 mM DTT) plus the protease inhibitors leupeptin and aprotinin. Purified and dialyzed proteins were aliquoted and stored at −80°C. Prior to use, all proteins were checked for purity and lack of proteolytic degradation by SDS-PAGE and Coomassie Blue staining.

In Vitro Nuclear Import Assays

Nuclear import assays were performed according to previously established protocols (Angeline et al., 2003; Knapp et al., 2009; Piccioli et al., 2010). Subconfluent HeLa cells, grown on 12 mm poly-L-lysine coated glass coverslips for 24 h, were permeablized with 70 g/ l digitonin for 5 min on ice to selectively permeabilize the plasma membrane while leaving the nuclear envelope intact. As a result, these digitoninpermeabilized cells will retain intact import-competent nuclei while being largely depleted of cytosolic transport factors. After three washes with cold transport buffer, the permeabilized cells were incubated with the import mixture for 30 min. Each import mixture contained an energy regenerating system (1 mM GTP, 1 mM ATP, 5 mM phosphocreatine, and 0.4U creatine phosphokinase) and the different GST fusion proteins (as indicated in the figure legend). In addition, each import contained either 3 ng/ l BSA in transport buffer, or HeLa cytosol. Final import reaction volumes were adjusted to 20 l with transport buffer.

For visualization of nuclear import, the GST fusion proteins were detected by immunofluorescence with a goat anti-GST antibody. Briefly, cells were washed, then fixed with 3.7% formaldehyde in PBS for 10 min on ice followed by methanol treatment for 3 min at −20°C. To reduce non-specific antibody binding the fixed cells were blocked for 1 h with 3% BSA/0.1% Tween in PBS. Cells were then incubated for 1 h with a 1:200 dilution of goat anti-GST primary antibody and after three washes with 3% BSA/0.1% Tween, cells were incubated with a 1:100 dilution of FITC conjugated rabbit anti-goat secondary antibody for 30 min. Following a final three washes, the coverslips were mounted using Vectashield-DAPI mounting medium to identify the nuclei by DAPI staining. Nuclear import was assessed by confocal fluorescence microscopy using a Leica TCS Sp5 broadband confocal microscope and representative images were taken using the Leica LAS AF software.

Preparation of GST-Nup62N and GST-Nup62C

The GST-Nup62N (containing aa 1-265 of Nup62), and GST-Nup62C (containing aa 178-522 of Nup62) plasmids (Zhong et al., 2005) were kindly provided by Dr. Nabeel

Yaseen. For protein expression and purification the GST-Nup62N, GST-Nup62C and GST plasmids were used to transform *E. coli BL21 CodonPlus*. After induction of the bacteria with 1mM IPTG for 3 h, GST-Nup62N, GST-Nup62C and GST were purified in their native state on Glutathione-Sepharose beads using a standard procedure.

Isolation assays

Before performing the binding assays, GST-Nup62N, GST-Nup62C and GST immobilized on glutathione- Sepharose were analyzed by SDS-PAGE and Coomassie staining. This analysis revealed for GST-Nup62N and GST-Nup62C the presence of the intact protein, and also some degradation. HeLa cell lysates containing the expressed EGFP-16E7, EGFP-16E7$_{LRLCV65AAAAA}$, EGFP-16E7$_{R66A}$, and EGFP (negative control) were incubated with GST-Nup62N (containing the FG domain of Nup62), GST-Nup62C (lacking any FG repeats) or with GST immobilized on glutathione-Sepharose for 1 h at 4°C. After washing the beads to remove nonspecific binding the bound proteins were analyzed by immunobloting with a GFP antibody. As a positive control for binding to Nup62N, we analyzed the binding of Kap β2 nuclear import receptor to GST-Nup62N by incubating HeLa cell lysate with GST-Nup62N, GST-Nup62C, or GST and the bound proteins were analyzed by immunobloting with a Kap β2 antibody.

Acknowledgments

We thank Dr. Nabeel Yaseen for the GST-Nup62N and GST-Nup62C plasmids. We thank Rebeca Cardoso, Courtney McKee and Aditya Ashok for help with purification of GST-fusion proteins. This work was supported by a grant from the National Institutes of Health (R01 CA94898) to Junona Moroianu.

Abbreviations

HPV	human papillomavirus
NLS	nuclear localization signal
NES	nuclear export signal
NPC	nuclear pore complex
EGFP	enhanced green fluorescent protein
GST	Glutathione-S-transferase

References

Angeline M, Merle E, Moroianu J. The E7 oncoprotein of high-risk human papillomavirus type 16 enters the nucleus via a nonclassical Ran-dependent pathway. Virology. 2003; 317:13–23. [PubMed: 14675621]

Avvakumov N, Torchia J, Mymryk JS. Interaction of the HPV E7 proteins with the pCAF acetyltransferase. Oncogene. 2003; 22:3833–3841. [PubMed: 12813456]

Bordeaux J, Forte S, Harding E, Darshan MS, Klucevsek K, Moroianu J. The l2 minor capsid protein of low-risk human papillomavirus type 11 interacts with host nuclear import receptors and viral DNA. J Virol. 2006; 80:8259–8262. [PubMed: 16873281]

Brehm A, Nielsen SJ, Miska EA, McCance DJ, Reid JL, Bannister AJ, Kouzarides T. The E7 oncoprotein associates with Mi2 and histone deacetylase activity to promote cell growth. The EMBO journal. 1999; 18:2449–2458. [PubMed: 10228159]

Darshan MS, Lucchi J, Harding E, Moroianu J. The l2 minor capsid protein of human papillomavirus type 16 interacts with a network of nuclear import receptors. J Virol. 2004; 78:12179–12188. [PubMed: 15507604]

Doorbar J. Molecular biology of human papillomavirus infection and cervical cancer. Clin Sci (Lond). 2006; 110:525–541. [PubMed: 16597322]

Helt AM, Funk JO, Galloway DA. Inactivation of both the retinoblastoma tumor suppressor and p21 by the human papillomavirus type 16 E7 oncoprotein is necessary to inhibit cell cycle arrest in human epithelial cells. Journal of virology. 2002; 76:10559–10568. [PubMed: 12239337]

Helt AM, Galloway DA. Destabilization of the retinoblastoma tumor suppressor by human papillomavirus type 16 E7 is not sufficient to overcome cell cycle arrest in human keratinocytes. Journal of virology. 2001; 75:6737–6747. [PubMed: 11435552]

Huh K, Zhou X, Hayakawa H, Cho JY, Libermann TA, Jin J, Harper JW, Munger K. Human papillomavirus type 16 E7 oncoprotein associates with the cullin 2 ubiquitin ligase complex, which contributes to degradation of the retinoblastoma tumor suppressor. Journal of virology. 2007; 81:9737–9747. [PubMed: 17609271]

Huh KW, DeMasi J, Ogawa H, Nakatani Y, Howley PM, Munger K. Association of the human papillomavirus type 16 E7 oncoprotein with the 600-kDa retinoblastoma protein-associated factor, p600. Proc Natl Acad Sci U S A. 2005; 102:11492–11497. [PubMed: 16061792]

Klucevsek K, Daley J, Darshan MS, Bordeaux J, Moroianu J. Nuclear import strategies of high-risk HPV18 L2 minor capsid protein. Virology. 2006; 352:200–208. [PubMed: 16733063]

Knapp AA, McManus PM, Bockstall K, Moroianu J. Identification of the nuclear localization and export signals of high risk HPV16 E7 oncoprotein. Virology. 2009; 383:60–68. [PubMed: 18996550]

Le Roux LG, Moroianu J. Nuclear entry of high-risk human papillomavirus type 16 E6 oncoprotein occurs via several pathways. J Virol. 2003; 77:2330–2337. [PubMed: 12551970]

Liu X, Clements A, Zhao K, Marmorstein R. Structure of the human Papillomavirus E7 oncoprotein and its mechanism for inactivation of the retinoblastoma tumor suppressor. J Biol Chem. 2006; 281:578–586. [PubMed: 16249186]

McKee CH, Onder Z, Ashok A, Cardoso R, Moroianu J. Characterization of the transport signals that mediate the nucleocytoplasmic traffic of low risk HPV11 E7. Virology. 2013

McLaughlin-Drubin ME, Huh KW, Munger K. Human papillomavirus type 16 E7 oncoprotein associates with E2F6. Journal of virology. 2008; 82:8695–8705. [PubMed: 18579589]

McLaughlin-Drubin ME, Munger K. The human papillomavirus E7 oncoprotein. Virology. 2009; 384:335–344. [PubMed: 19007963]

Munger K, Baldwin A, Edwards KM, Hayakawa H, Nguyen CL, Owens M, Grace M, Huh K. Mechanisms of human papillomavirus-induced oncogenesis. J Virol. 2004; 78:11451–11460. [PubMed: 15479788]

Naim B, Zbaida D, Dagan S, Kapon R, Reich Z. Cargo surface hydrophobicity is sufficient to overcome the nuclear pore complex selectivity barrier. Embo J. 2009; 28:2697–2705. [PubMed: 19680225]

Nelson LM, Rose RC, Moroianu J. Nuclear import strategies of high risk HPV16 L1 major capsid protein. J Biol Chem. 2002; 23:23.

Nguyen CL, Munger K. Human papillomavirus E7 protein deregulates mitosis via an association with nuclear mitotic apparatus protein 1. J Virol. 2009; 83:1700–1707. [PubMed: 19052088]

Piccioli Z, McKee CH, Leszczynski A, Onder Z, Hannah EC, Mamoor S, Crosby L, Moroianu J. The nuclear localization of low risk HPV11 E7 protein mediated by its zinc binding domain is independent of nuclear import receptors. Virology. 2010; 407:100–109. [PubMed: 20800258]

Roman A, Munger K. The papillomavirus E7 proteins. Virology. 2013

Solmaz SR, Chauhan R, Blobel G, Melcak I. Molecular architecture of the transport channel of the nuclear pore complex. Cell. 2011; 147:590–602. [PubMed: 22036567]

Terry LJ, Wente SR. Flexible gates: dynamic topologies and functions for FG nucleoporins in nucleocytoplasmic transport. Eukaryot Cell. 2009; 8:1814–1827. [PubMed: 19801417]

Tsuji T, Sheehy N, Gautier VW, Hayakawa H, Sawa H, Hall WW. The nuclear import of the human T lymphotropic virus type I (HTLV-1) tax protein is carrier and energy-independent. J Biol Chem. 2007; 282:13875–13883. [PubMed: 17344183]

Zhong H, Takeda A, Nazari R, Shio H, Blobel G, Yaseen NR. Carrier-independent nuclear import of the transcription factor PU.1 via RanGTP-stimulated binding to Nup153. J Biol Chem. 2005; 280:10675–10682. [PubMed: 15632149]

zur Hausen H. Papillomaviruses causing cancer: evasion from host-cell control in early events in carcinogenesis. J Natl Cancer Inst. 2000; 92:690–698. [PubMed: 10793105]

zur Hausen H. Papillomaviruses in the causation of human cancers - a brief historical account. Virology. 2009; 384:260–265. [PubMed: 19135222]

Highlights

➢ An intact zinc-binding domain is essential for the nuclear localization of HPV16 E7

➢ Identification of a hydrophobic patch that is critical for the nuclear import of HPV16 E7

➢ HPV16 E7 interacts via its zinc-binding domain with the FG domain of Nup62

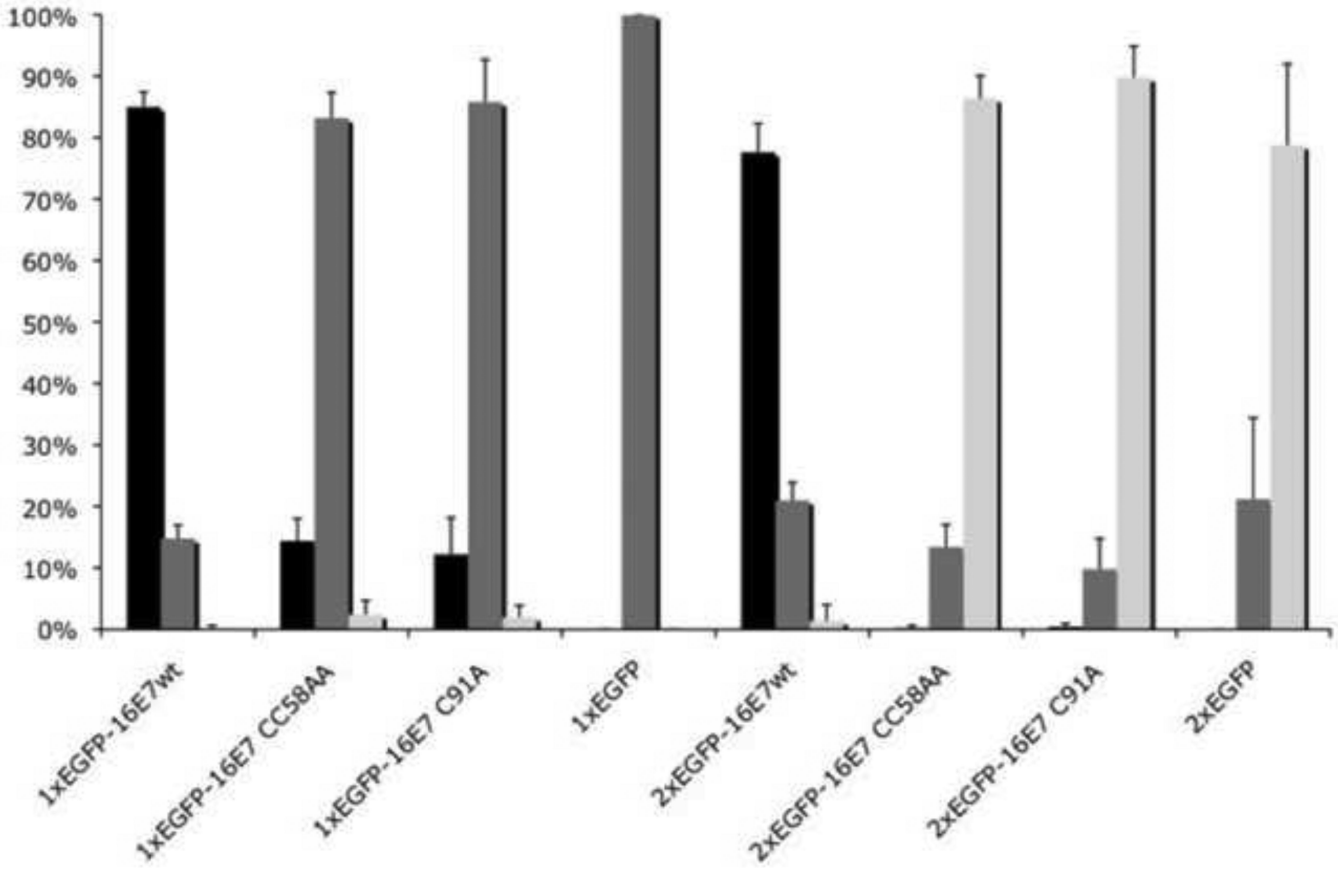

Fig. 1. Quantitative analysis of the effect of mutations of the zinc coordinating cysteine residues to alanine on the nuclear localization of EGFP-16E7 and 2xEGFP-16E7

Data from five experiments using EGFP-16E7, EGFP-16E7$_{CC58AA}$, EGFP-16E7$_{C91A}$, EGFP, 2xEGFP-16E7, 2xEGFP-16E7$_{CC58AA}$, 2xEGFP-16E7$_{C91A}$, and 2xEGFP plasmids were used for quantitative analysis and graphic representation of the localization distribution of transfected HeLa cells. Black bars represent cells exhibiting predominant nuclear localization; gray bars represent cells exhibiting pancellular localization; white bars represent cells exhibiting predominant cytoplasmic localization.

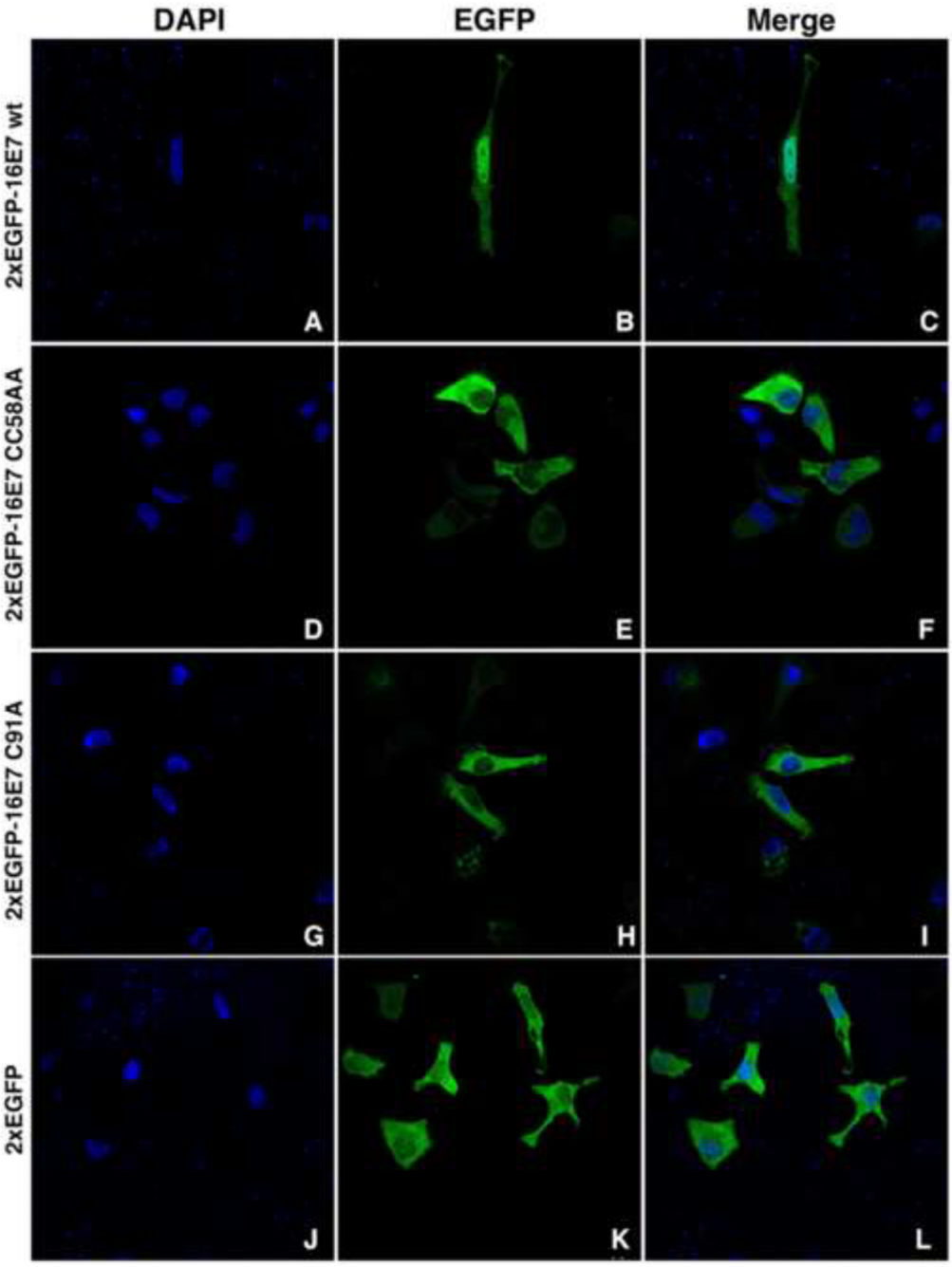

Fig. 2. Mutation of the zinc coordinating cysteine residues to alanine changes the nuclear localization of 2xEGFP-16E7

HeLa cells were transfected with either 2xEGFP-16E7 wild type (panels A-C), 2xEGFP-16E7$_{CC58AA}$ (panels D-F), 2xEGFP-16E7$_{C91A}$ (panels G-I), or 2xEGFP (panels J-L) plasmids and examined by confocal fluorescence microscopy at 24 h post transfection. Panels A, D, G and J represent the DAPI staining of the nuclei, panels B, E, H and K represent the fluorescence of the EGFP and panels C, F, I, and L represent the merge.

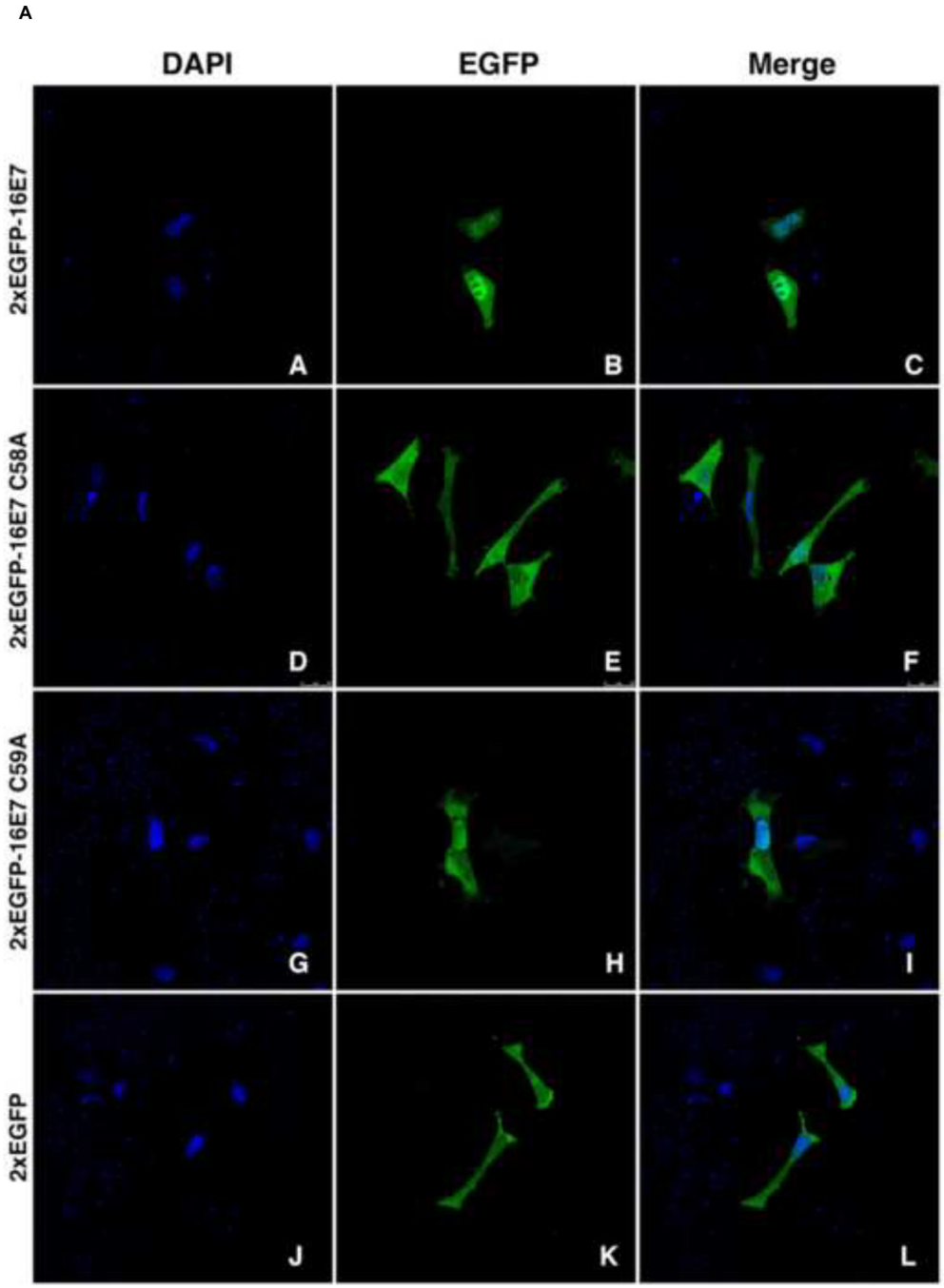

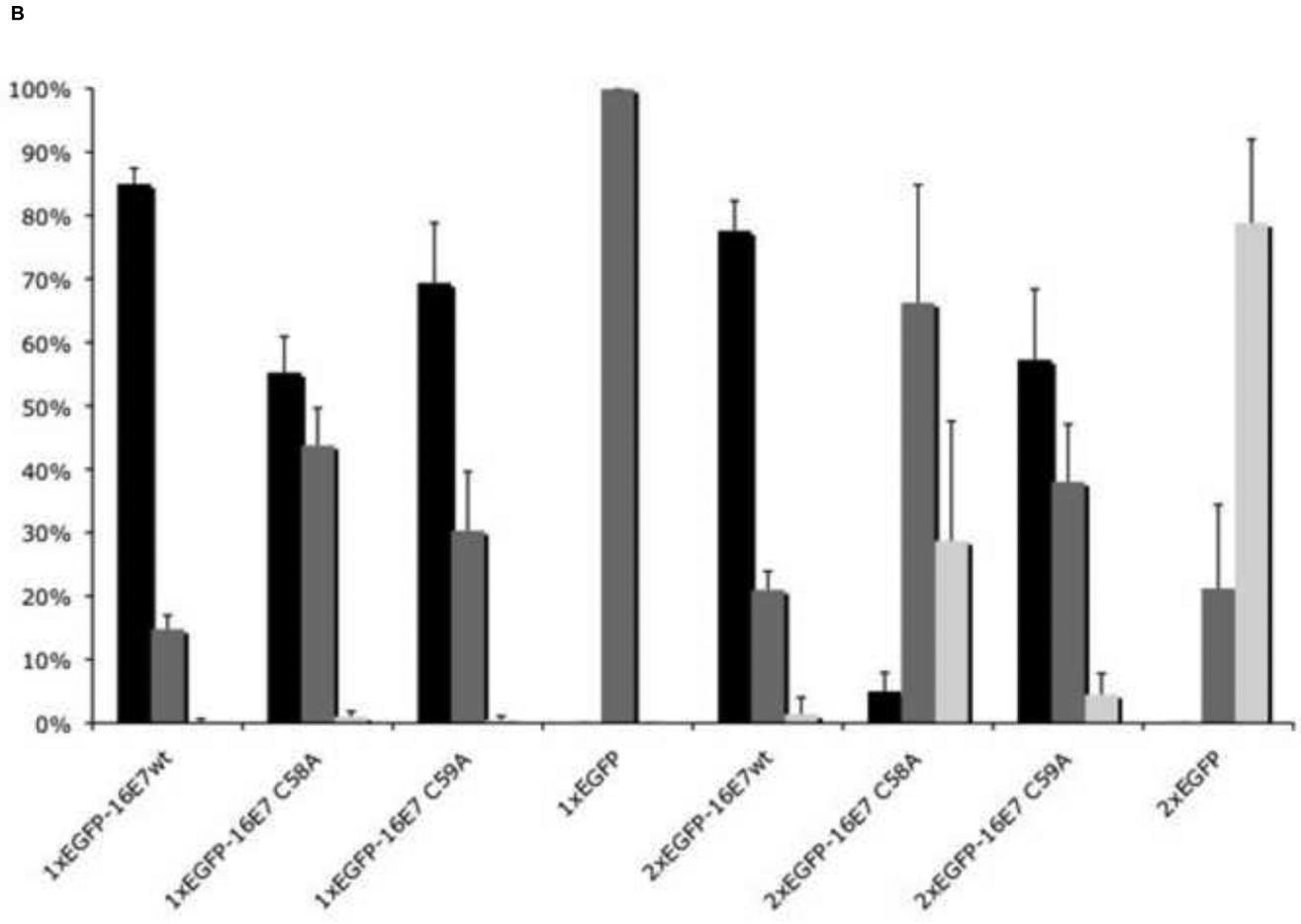

Fig. 3.

A. Single cysteine substitution to alanine within the zinc finger alters the nuclear localization of 2xEGFP-16E7. HeLa cells were transfected with either 2xEGFP-16E7 wild type (panels A-C), 2xEGFP-16E7$_{C58A}$ (panels D-F), 2xEGFP-16E7$_{C59A}$ (panels G-I), or 2xEGFP (panels J-L) plasmids and examined by confocal fluorescence microscopy at 24 h post-transfection. Panels A, D, G and J show the DAPI staining of the nuclei, panels B, E, H and K represent the fluorescence of the EGFP and panels C, F, I, and L represent the merge. B. Quantitative analysis of the effect of single cysteine substitution within the zinc finger on the localization of EGFP-16E7 and 2xEGFP-16E7. Data from five experiments using EGFP-16E7, EGFP-16E7$_{C58A}$, EGFP-16E7$_{C59A}$, EGFP, 2xEGFP-16E7, 2xEGFP-16E7$_{C58A}$, 2xEGFP-16E7$_{C59A,}$ and 2xEGFP plasmids were used for quantitative analysis and graphic representation of the localization distribution of transfected HeLa cells. Black bars represent cells exhibiting predominant nuclear localization; gray bars represent cells exhibiting pancellular localization; white bars represent cells exhibiting predominant cytoplasmic localization.

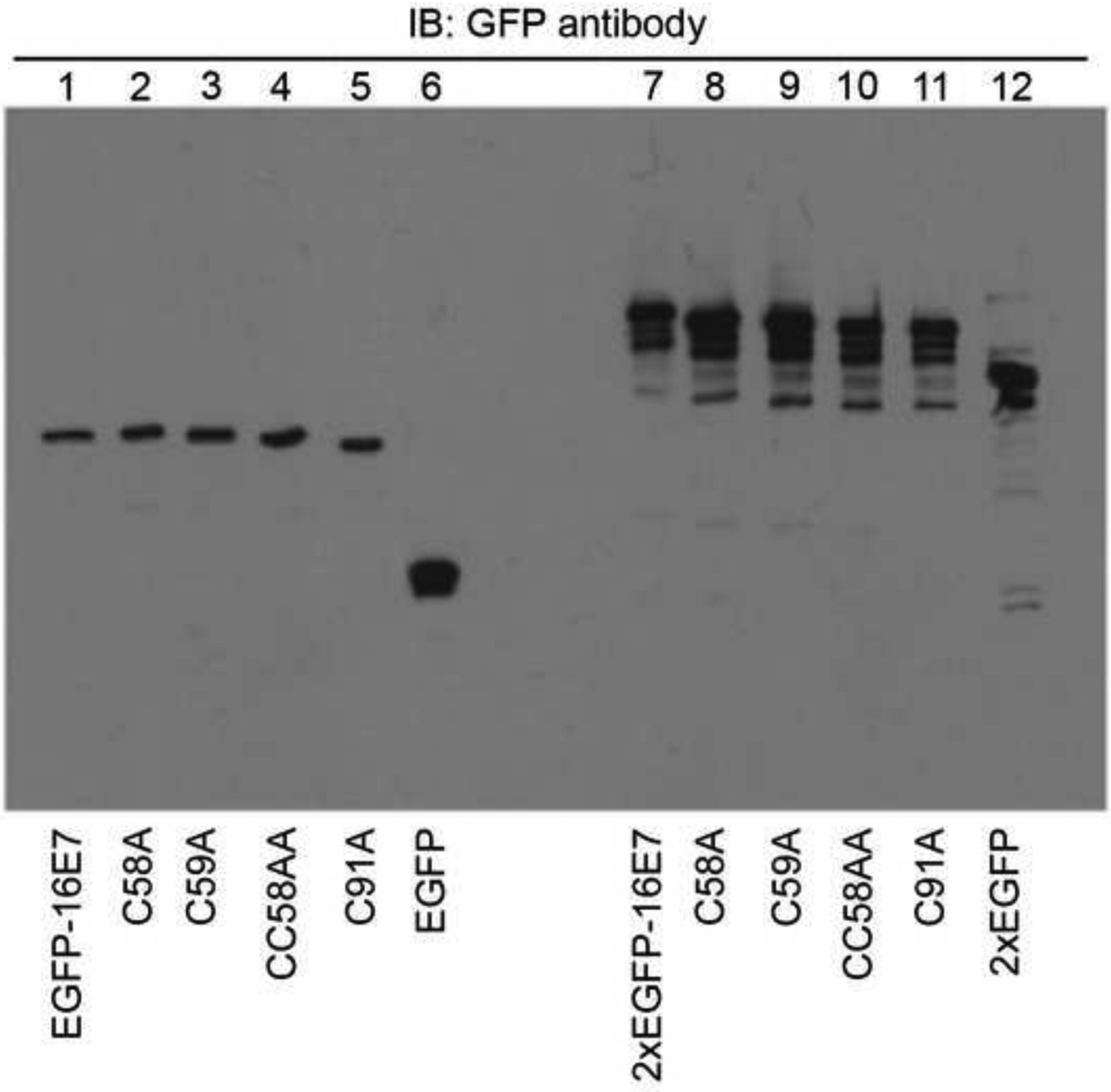

Fig. 4. The EGFP-16E7 and 2xEGFP-16E7 cysteine mutants are properly expressed in HeLa cells

HeLa cells were transfected with EGFP-16E7 (lane 1), EGFP-16E7$_{C58A}$ (lane 2), EGFP-16E7$_{C59A}$ (lane 3), EGFP-16E7$_{CC58AA}$ (lane 4), EGFP-16E7$_{C91A}$ (lane 5), EGFP (lane 6), 2xEGFP-16E7 (lane 7), 2xEGFP-16E7$_{C58A}$ (lane 8), 2xEGFP-16E7$_{C59A}$ (lane 9), 2xEGFP-16E7$_{CC58AA}$ (lane 10), 2xEGFP-16E7$_{C91A}$ (lane 11), or 2xEGFP (lane 12) plasmids. Cell lysates were prepared 24 h post transfection and probed with a GFP antibody.

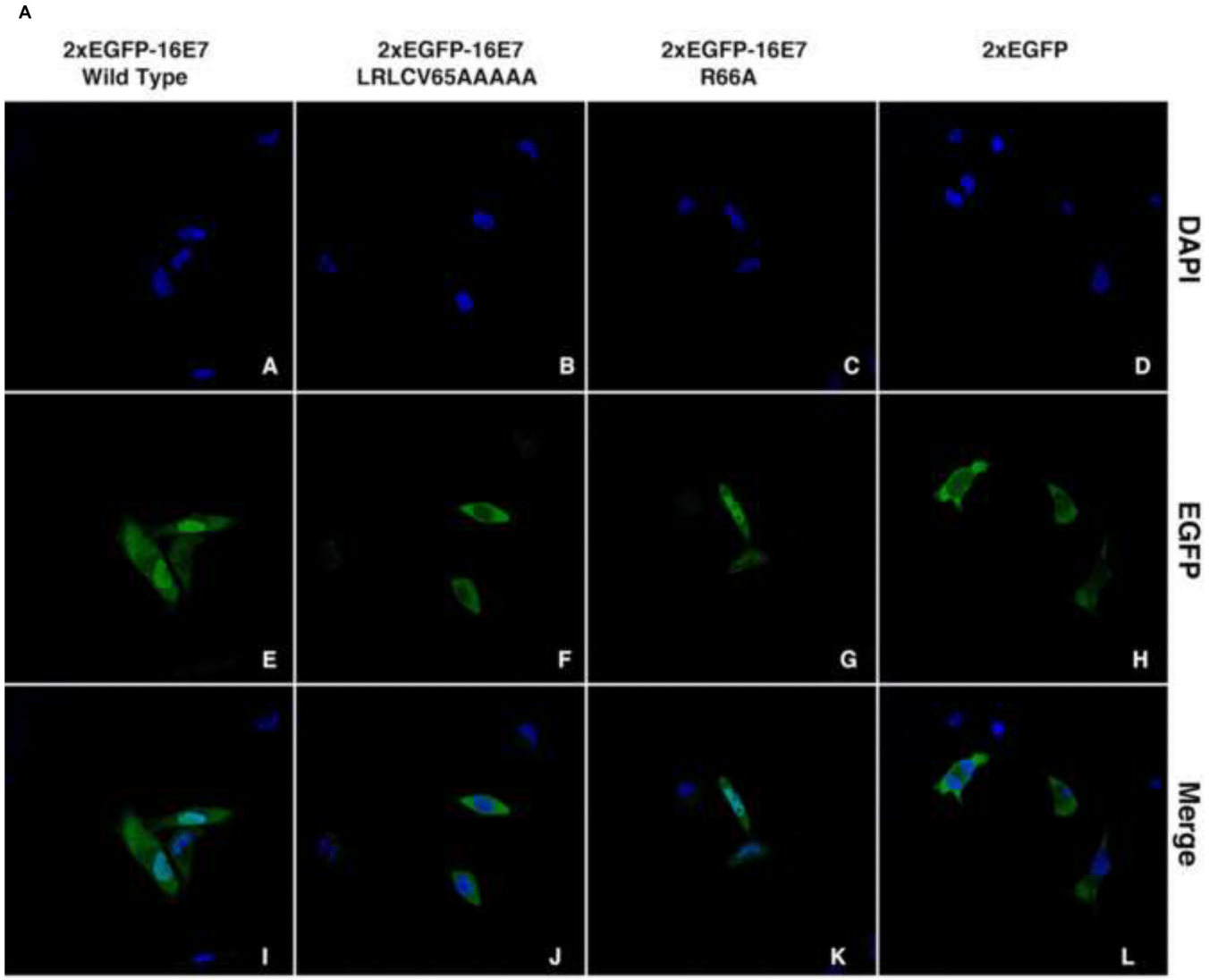

B

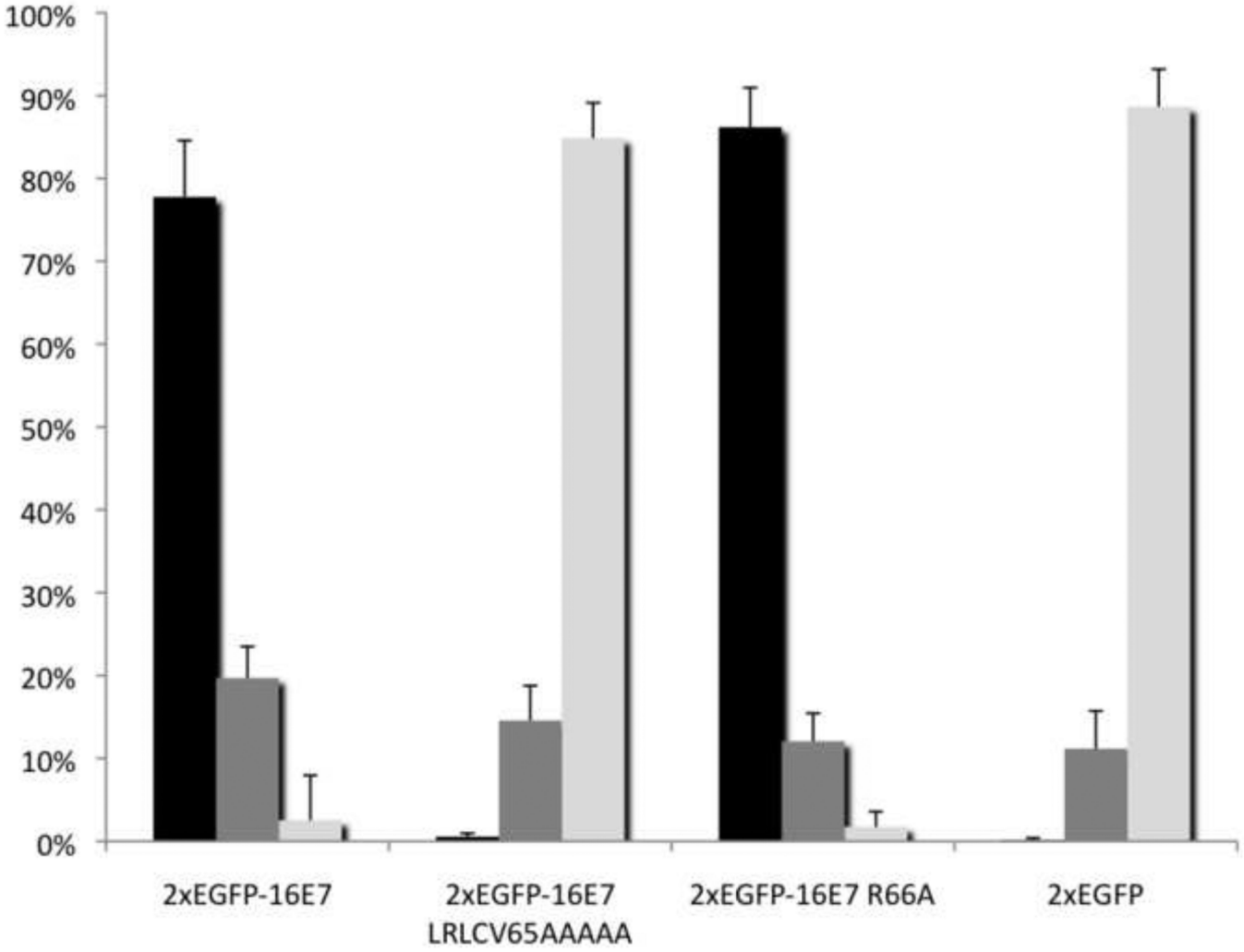

C

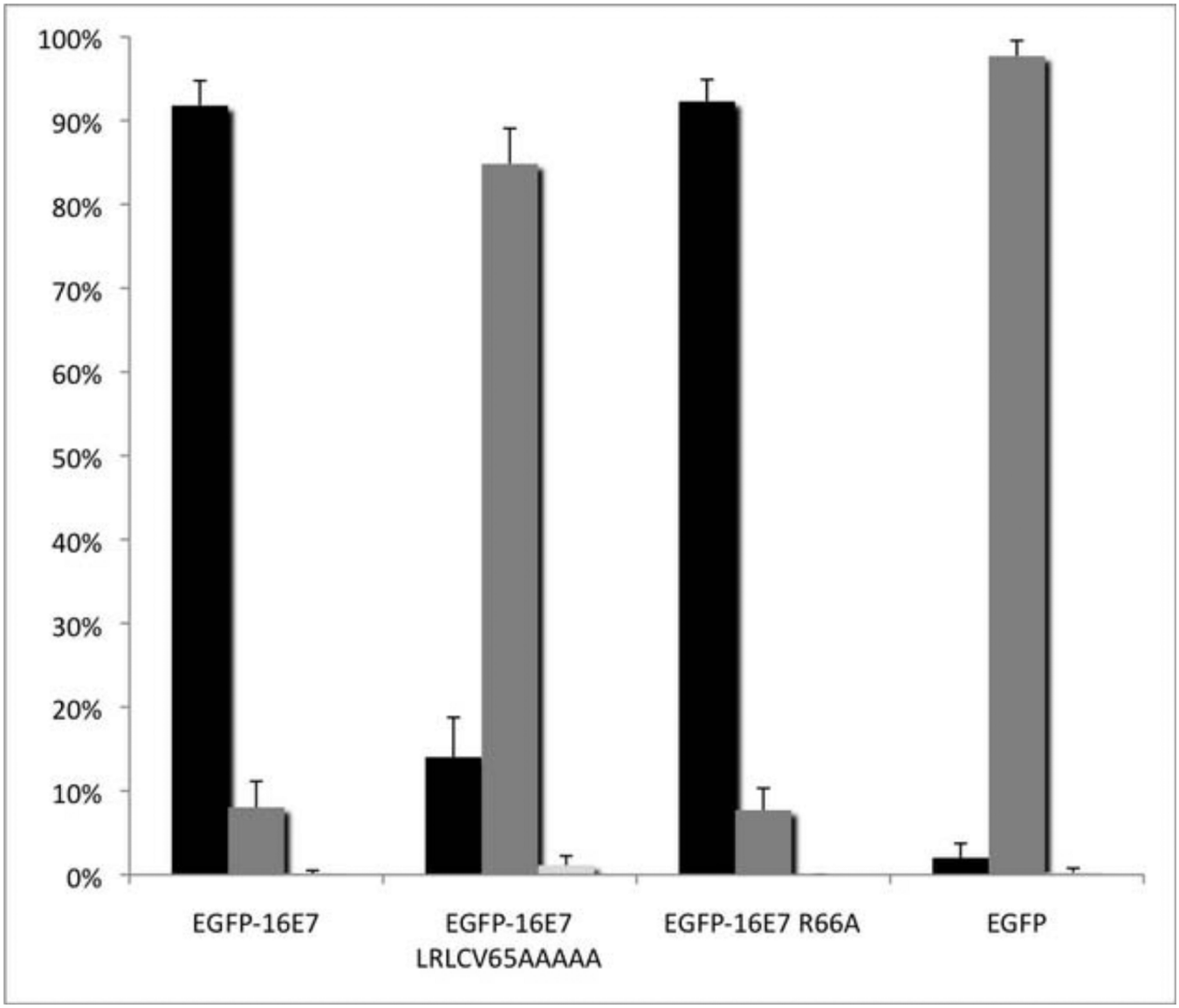

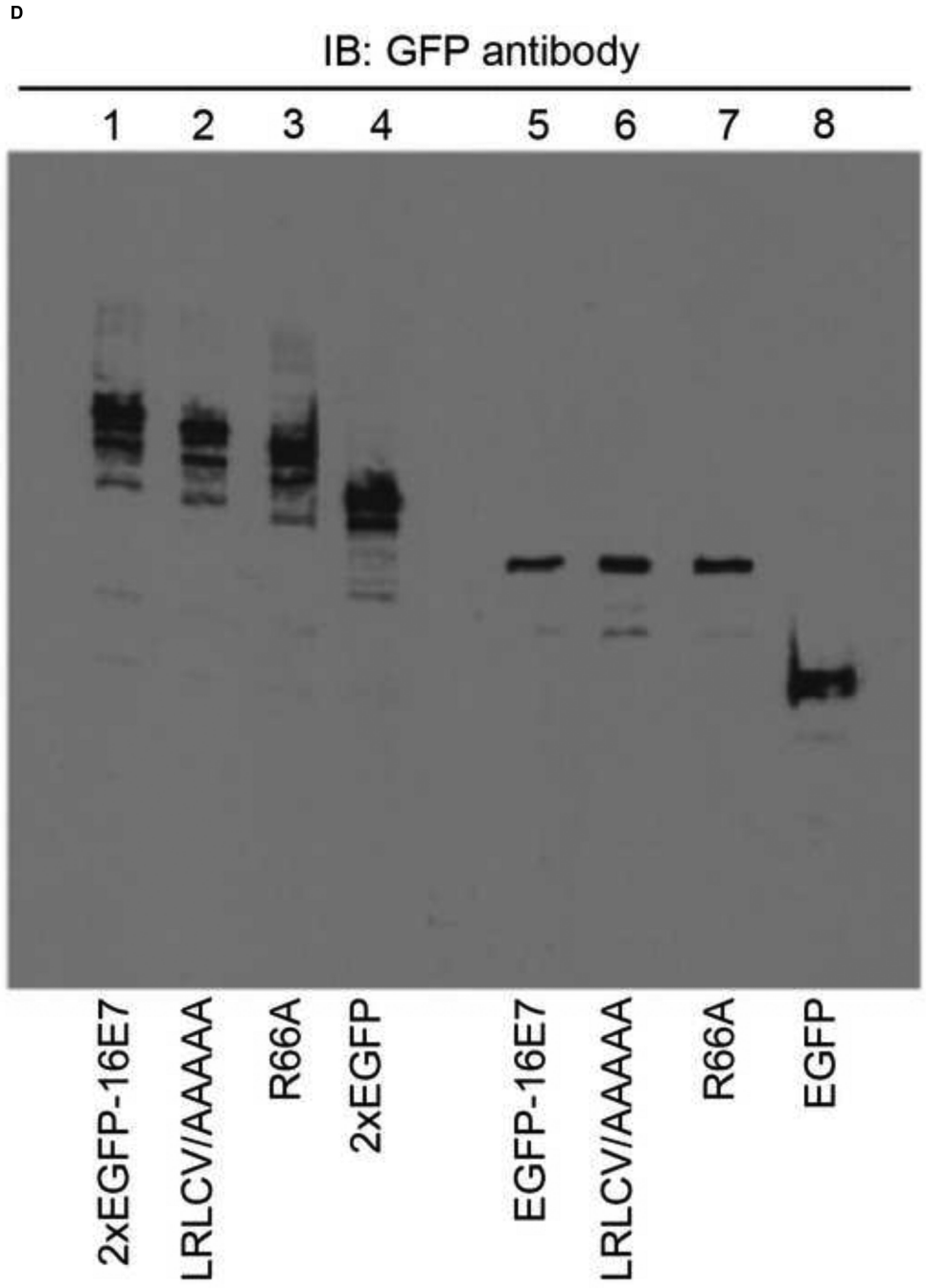

Fig. 5.

A. Mutation of hydrophobic residues within the zinc-binding domain disrupts the nuclear localization of 2xEGFP-16E7. HeLa cells were transfected with either 2xEGFP-16E7 wild type (panels A, E, and I), 2xEGFP-16E7$_{LRLCV65AAAAA}$ (panels B, F, and J), 2xEGFP-16E7$_{R66A}$ (panels C, G, and K), or 2xEGFP (panels D, H, and L) plasmids and examined by confocal fluorescence microscopy at 24 h post-transfection. Panels A-D represent DAPI staining of the nuclei, panels E-H represent EGFP fluorescence, and panels I-L represent the merge. B. Quantitative analysis of the effect of mutation of hydrophobic residues within the zinc-binding domain on the localization of 2xEGFP-16E7 in HeLa cells. Data from seven experiments using 2xEGFP-16E7 wild type,

2xEGFP-16E7$_{LRLCV65AAAAA}$, 2xEGFP-16E7$_{R66A}$, and 2xEGFP plasmids were used for quantitative analysis and graphic representation of the localization distribution of transfected HeLa cells. Black bars represent cells exhibiting predominant nuclear localization; gray bars represent cells exhibiting pancellular localization; white bars represent cells exhibiting predominant cytoplasmic localization. C. Quantitative analysis of the effect of mutation of hydrophobic residues within the zinc-binding domain on the localization of EGFP-16E7 in HeLa cells. Data from five experiments using EGFP-16E7 wild type, EGFP-16E7$_{LRLCV65AAAAA}$, EGFP-16E7$_{R66A}$, and EGFP plasmids were used for quantitative analysis and graphic representation of the localization distribution of transfected HeLa cells. Black bars represent cells exhibiting predominant nuclear localization; gray bars represent cells exhibiting pancellular localization; white bars represent cells exhibiting predominant cytoplasmic localization. D. EGFP-16E7 and 2xEGFP-16E7 hydrophobic residues and R66A mutants are properly expressed in HeLa cells. HeLa cells were transfected with 2xEGFP-16E7 (lane 1), 2xEGFP-16E7$_{LRLCV65AAAAA}$ (lane 2), 2xEGFP-16E7$_{R66A}$ (lane 3), 2xEGFP (lane 4), EGFP-16E7 (lane 5), EGFP-16E7$_{LRLCV65AAAAA}$ (lane 6), EGFP-16E7$_{R66A}$ (lane 7), or EGFP (lane 8) plasmids. Cell lysates were prepared 24 h post transfection and probed with a GFP antibody.

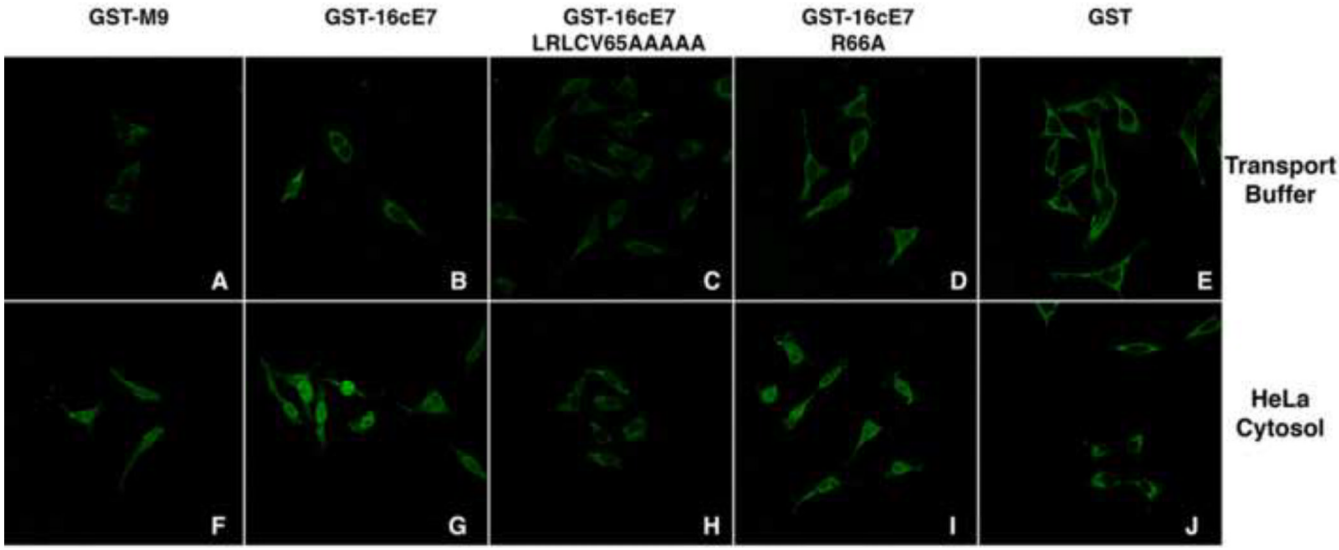

Fig. 6. Mutation of hydrophobic residues within the zinc-binding domain inhibits nuclear import of GST-16cE7

Digitonin-permeabilized HeLa cells were incubated with GST-M9 (panels A and F), GST-16cE7 (panels B and G), GST-16cE7$_{LRLCV65AAAAA}$ (panels C and H), GST-16cE7$_{R66A}$ (panels D and I), or GST (panels E and J) in the presence of only transport buffer (panels A-E) or HeLa cytosol and energy mix (panels F-J).

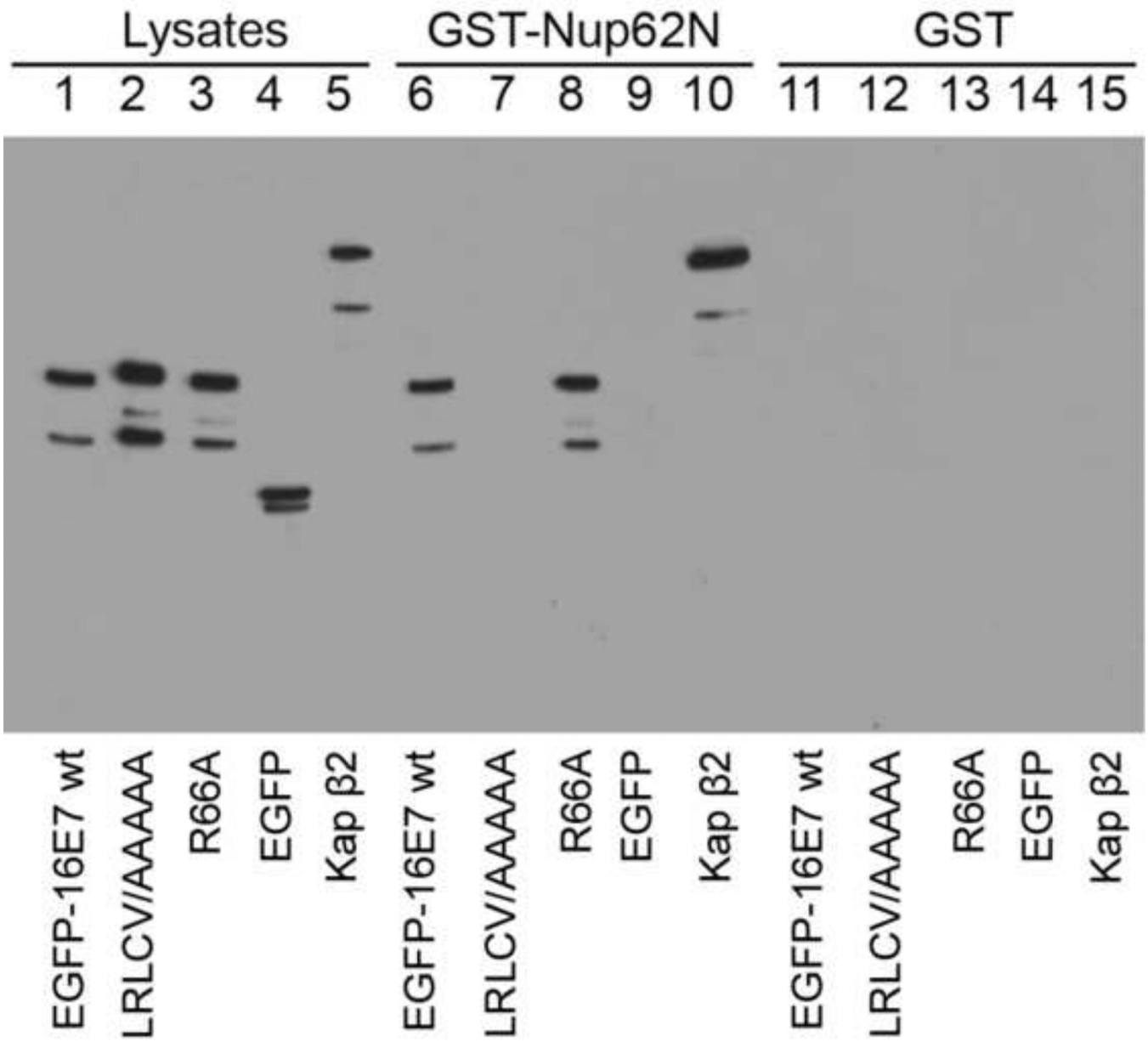

Fig. 7. HPV16 E7 interacts with the FG domain of Nup62 and mutations of hydrophobic residues within the zinc-binding domain disrupt this interaction

HeLa cells were transfected with EGFP-16E7, EGFP-16E7$_{LRLCV65AAAAA}$, EGFP-16E7$_{R66A}$, and EGFP plasmids. Cell lysates were prepared 24 h post transfection and probed with either a GFP antibody (lane 1, EGFP-16E7; lane 2, EGFP-16E7$_{LRLCV65AAAAA}$; lane 3, EGFP-16E7$_{R66A}$; lane 4, EGFP) or Kap 2 antibody (lane 5). GST-Nup62N (lanes 6-10) and GST (lanes 11-15) immobilized on glutathione-Sepharose were incubated with the cell lysates and the bound proteins were eluted and analyzed via immunoblotting with a GFP antibody (lanes 6 and 11, EGFP-16E7; lanes 7 and 12, EGFP-16E7 $_{LRLCV65AAAAA}$; lanes 8 and 13, EGFP-16E7$_{R66A}$; and lanes 9 and 14, EGFP). Binding of Kap 2 to GSTNup62N and GST was detected with a Kap 2 antibody (lanes 10 and 15).

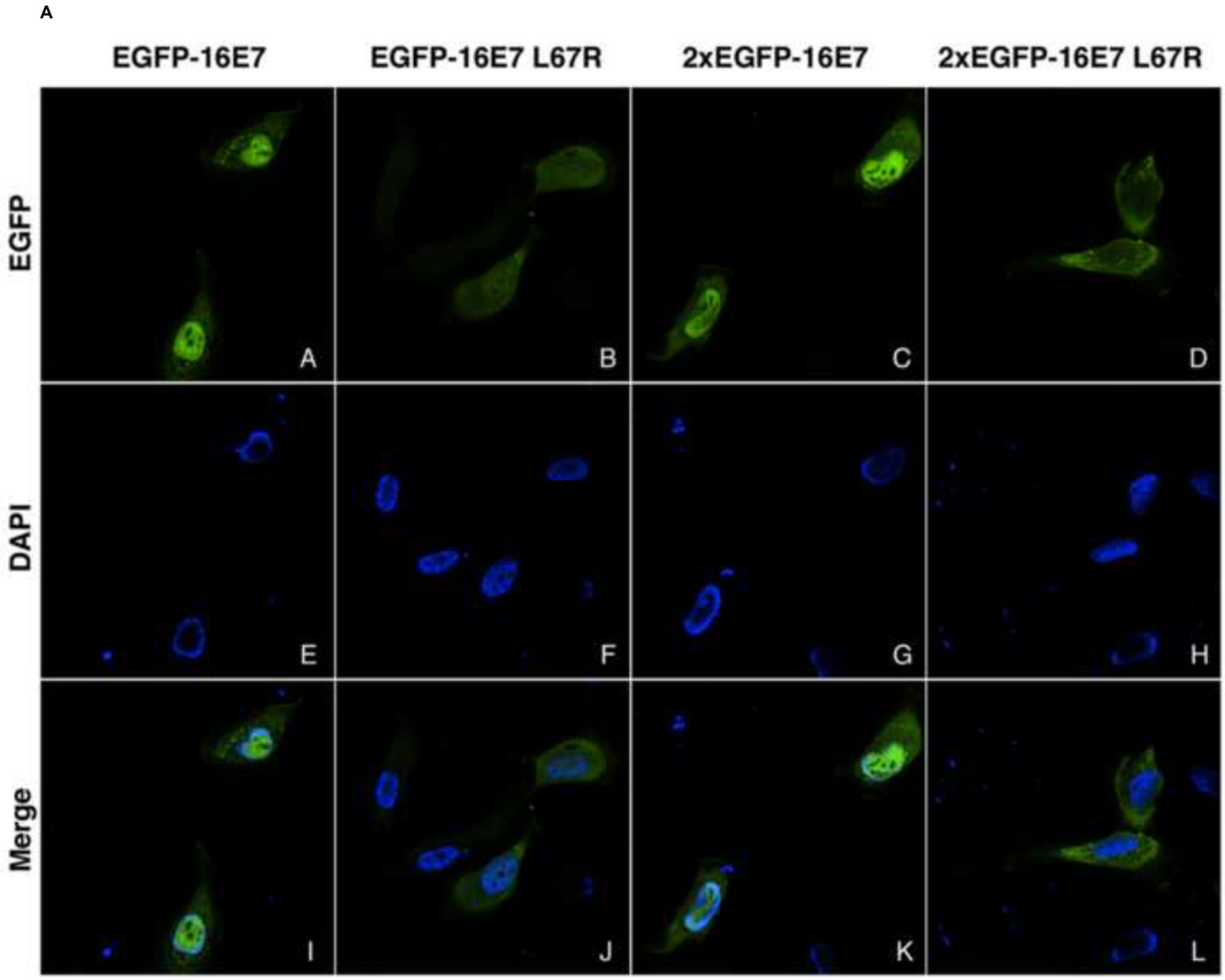

B

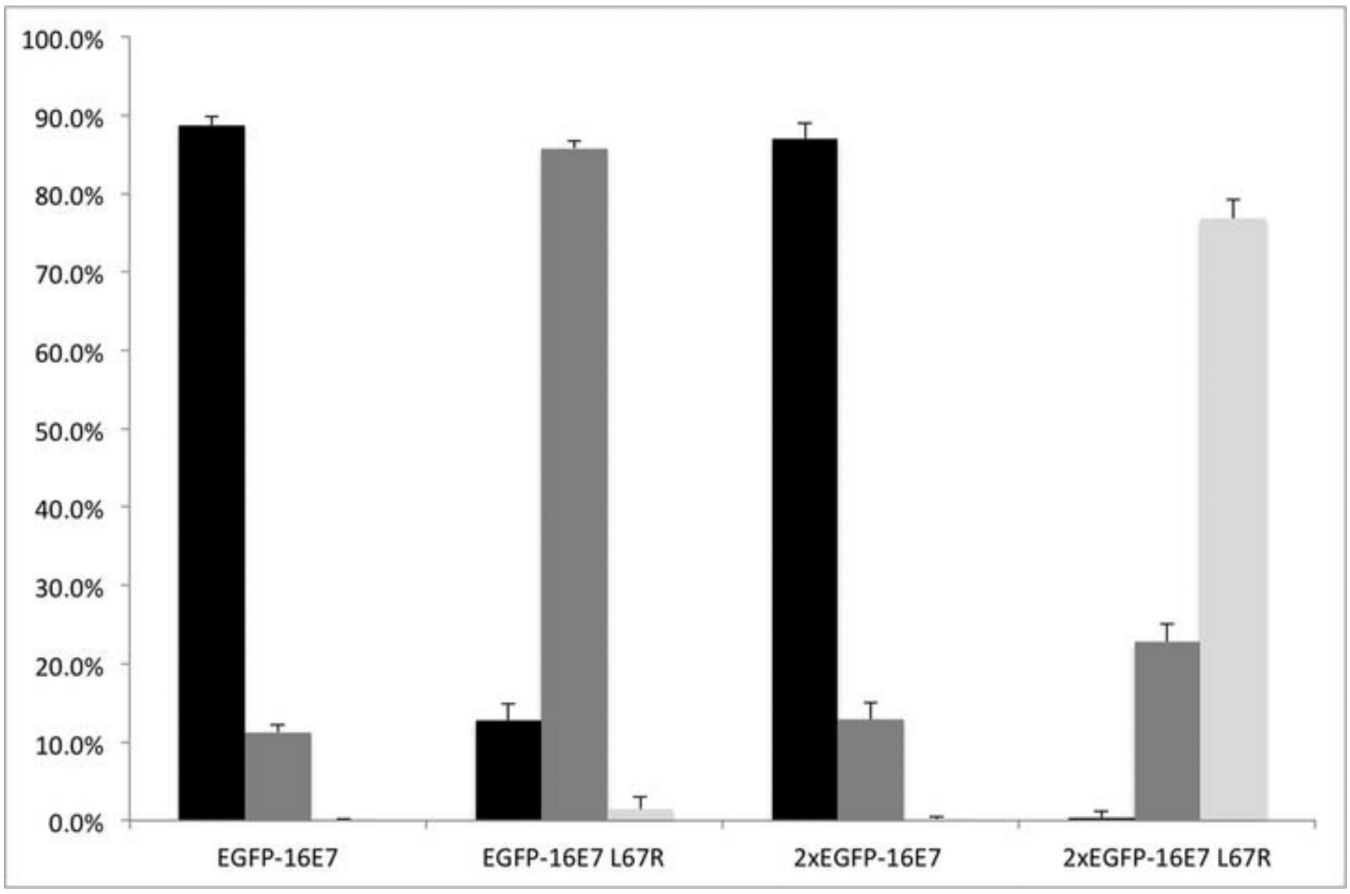

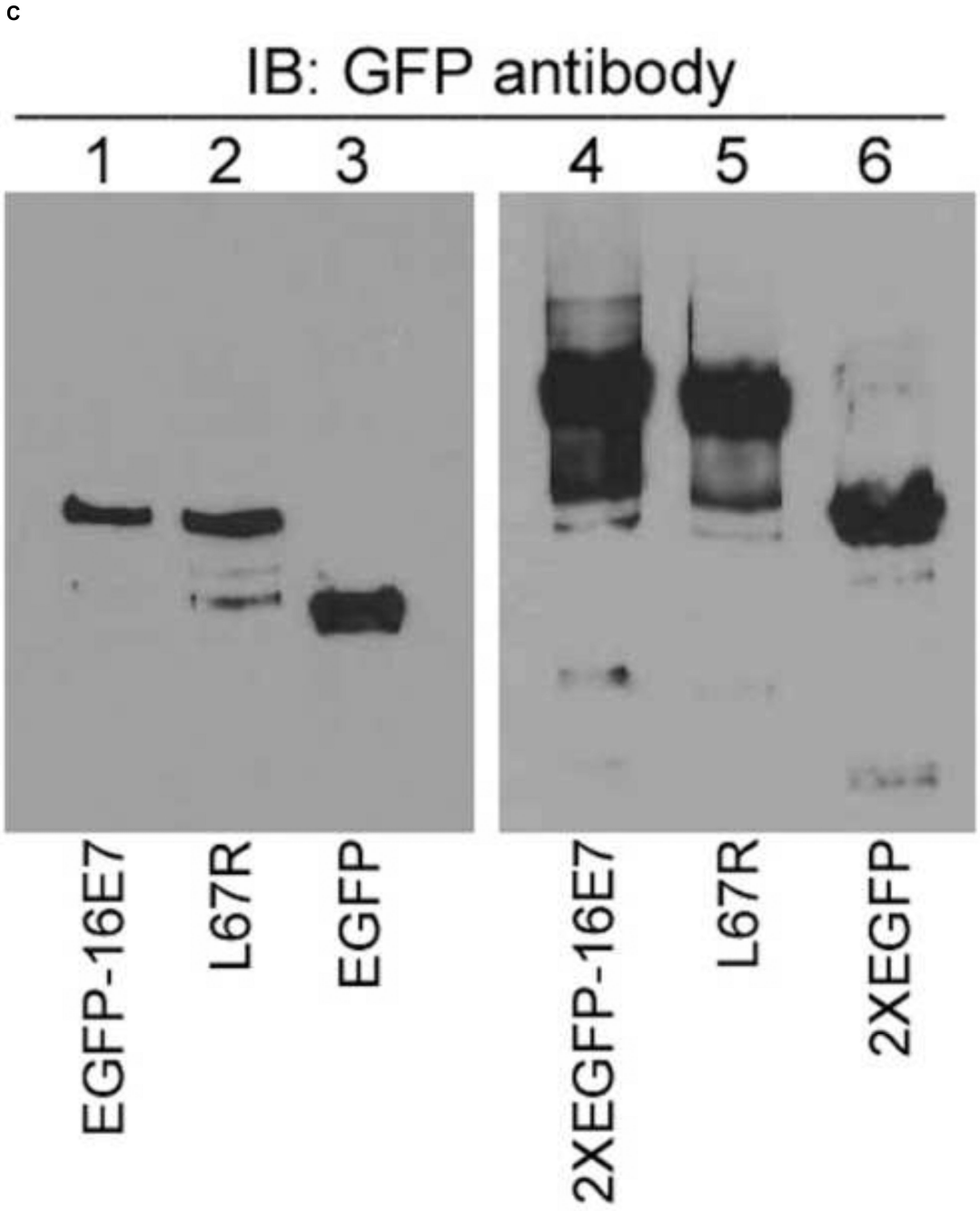

Fig. 8. The L67R mutation disrupts the nuclear localization of EGFP-16E7 and 2xEGFP-16E7

A. HeLa cells were transfected with EGFP-16E7 (panels A, E and I), EGFP-16E7$_{L67R}$ (panels B, F and J), 2xEGFP-16E7 (panels C, G and K), or 2xEGFP-16E7$_{L67R}$ (panels D, H and L) plasmids, and the localization of the expressed proteins was analyzed by confocal fluorescence microscopy. Panels A-D represent the fluorescence of the EGFP, panels E-H the DAPI staining of the nuclei, and panels I-L the merge. B. Quantitative analysis of the effect of L67R mutation on the localization of EGFP-16E7 and 2xEGFP-16E7. Data from four experiments using EGFP-16E7 wild type, EGFP-16E7$_{L67R}$, 2xEGFP-16E7 wild type and 2xEGFP-16E7$_{L67R}$ plasmids were used for the quantitative analysis and graphic

representation of the localization distribution of transfected HeLa cells. Black bars represent cells showing predominant nuclear localization; gray bars represent cells showing pancellular localization; white bars represent cells showing predominant cytoplasmic localization. C. EGFP-16E7$_{L67R}$ and 2xEGFP-16E7$_{L67R}$ mutants are properly expressed in HeLa cells. HeLa cells were transfected with EGFP-16E7 (lane 1), EGFP-16E7$_{\mathbf{L67R}}$ (lane 2), EGFP (lane 3), 2xEGFP-16E7 (lane 4), 2xEGFP-16E7$_{\mathbf{L67R}}$ (lane 5) and 2xEGFP (lane 6). Cell lysates were prepared 24 h post transfection and probed with a GFP antibody.

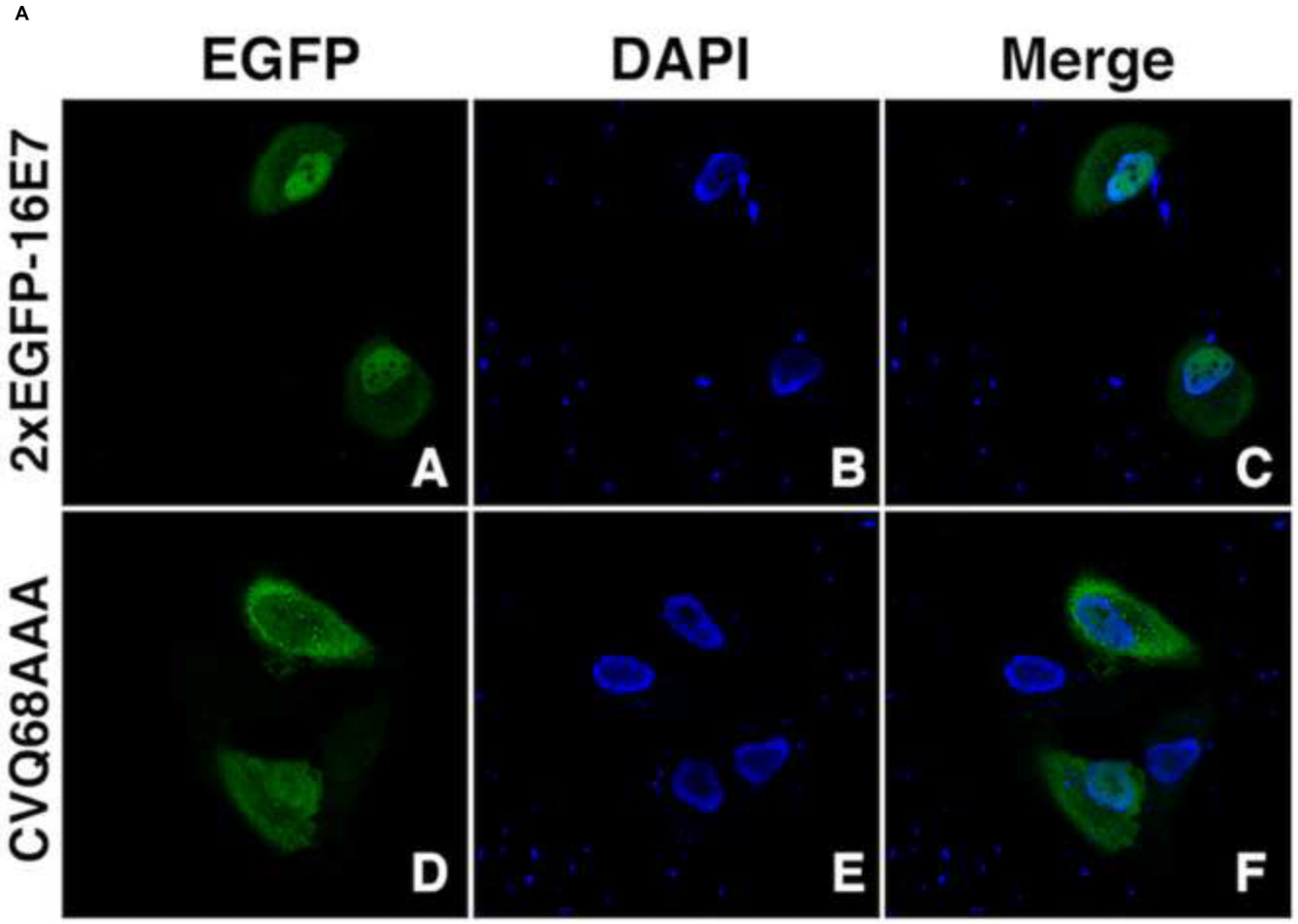

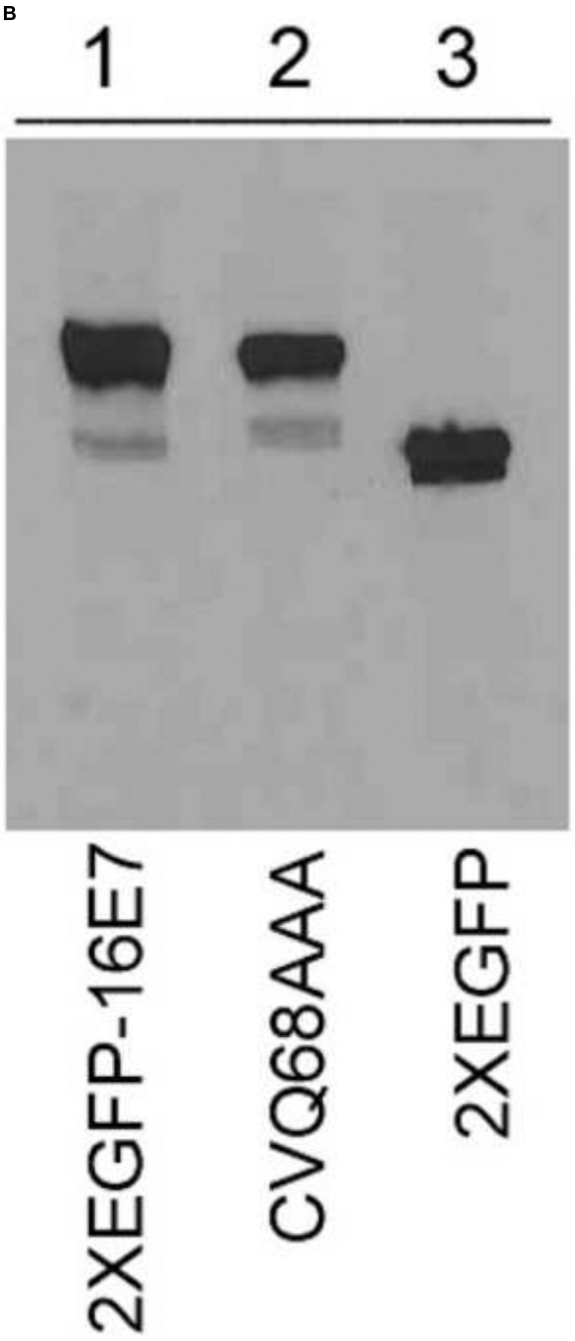

Fig. 9.

A. Analysis of the effect of CVQ68AAA mutation on the nuclear localization of 2xEGFP-16E7. HeLa cells were transfected with 2xEGFP-16E7 (panels A, B and C) or 2xEGFP-16E7$_{CVQ68AAA}$ (panels D, E and F) plasmids, and the localization of the expressed proteins was analyzed by confocal fluorescence microscopy. Panels A and D represent the fluorescence of the EGFP, panels B and E the DAPI staining of the nuclei, and panels C and F the merge. **B. The 2xEGFP-16E7$_{CVQ68AAA}$ mutant is expressed properly in HeLa cells.** HeLa cells were transfected with 2xEGFP-16E7 (lane 1), 2xEGFP-16E7$_{CVQ68AAA}$

(lane 2) and 2xEGFP (lane 3). Cell lysates were prepared 24 h post transfection and probed with a GFP antibody.